NASA CONTRACTOR REPORT

NASA CR-242

(O.K.)

60537

20010720 139

SOME CONSIDERATIONS IN THE FATIGUE DESIGN OF LAUNCH AND SPACECRAFT STRUCTURES

by R. H. Christensen and R. J. Bellinfante

Prepared under Contract No. NAS 7-298 *by*
DOUGLAS AIRCRAFT COMPANY, INC.
Santa Monica, Calif.

for

NATIONAL AERONAUTICS AND SPACE ADMINISTRATION • WASHINGTON, D. C. • JUNE 1965

NASA CR-242

SOME CONSIDERATIONS IN THE FATIGUE DESIGN

OF LAUNCH AND SPACECRAFT STRUCTURES

By R. H. Christensen and R. J. Bellinfante

Distribution of this report is provided in the interest of information exchange. Responsibility for the contents resides in the author or organization that prepared it.

NOTICES

FOREWORD

This NASA contract, "Some Considerations in the Fatigue Design
of Launch and Spacecraft Structures," was initiated under Project
No. NAS 7-298. The work was administered under the direction
of T. V. Cooney, OAR&T, NASA Headquarters, and H. F. Hardrath,
Structures Research Division, Langley Research Center, acting as
Principal Representatives.

The Douglas program was conducted under the direction of
R. W. Hallet, Jr., Director of Research and Development, Ad-
vance Systems and Technology, with R. H. Christensen acting as
Study Director.

CONTENTS

Preceding Page's Blank

FIGURES

SUMMARY

Five years ago, metal fatigue was considered by many to be
an unimportant problem in the design of space vehicle systems.
Within this period, potential problems were reviewed period-
ically as experience in the operation of these vehicles increased.
No fatigue design criteria have yet been formally documented for
this new class of vehicles. Now, trends in future space system
design, in addition to some current experience, dictate that the
problem can no longer be neglected. This report is intended to
supply background information useful in the design of space
vehicle system structures.

The report presents a definition of the fatigue problem as it
relates to the strength of structure. It briefly reviews present
knowledge in designing to prevent the occurrence of this unde-
sirable phenomenon. Current evaluation methods and guides
for use in design, test, and analysis are also reviewed.

Several appendixes appear at the end of the report. Their pur-
pose is to serve as a checklist for the designer on those aspects
of the problem that are often neglected or are not well known.
A review of the appendixes will also reveal those areas in which
additional research is required.

1

STATEMENT OF THE PROBLEM

The whole subject of fatigue of structures is concerned with the fact that during the operation of a vehicle, fatigue cracks can be formed within its stressed members; once initiated, these cracks may propagate to critical dimensions. Repetitive loads experienced throughout the useful life of a structure are the cause of this damaging phenomenon and the eventual generation of flaws. The mechanism is accumulative and decreases the strength of highly stressed components of a vehicle structure with their time in service. This undesirable situation can result in catastrophic consequences. Designing to prevent the occurrence of this phenomenon is therefore important if vehicles are to be economically built and yet possess adequate safety and construction that requires minimal repair.

In order to assure integrity of structure and a satisfactory life for vehicles, the spectra of loads and environments which the structure will encounter must be defined. The major load and environmental parameters requiring definition for the majority of vehicles, are those induced by wind, shock, vibration, engine exhaust noise, cycling, pressurization, kinetic heating, operational heating, and atmospheric corrosion. (The above conditions are applicable to space vehicle systems.)

Knowledge of the response of structure and of the behavior of materials of construction under these anticipated loads should then enable the designer to design safe vehicles. The normal practice has been to accomplish this task by accepted stress analysis methods in conjunction with laboratory fatigue tests on component parts. An alternate but far more costly procedure to evaluate fatigue resistance of structure is to fatigue-test the entire vehicle. Regardless of the method chosen, it will be possible to make valid assessments of fatigue life only through accurate simulation of the environment the vehicle will encounter. It often will be necessary to consider the effect on structure of combined environments. The effect of the many environments experienced during the operation of vehicles is time dependent and this factor cannot be overlooked. Large errors in the prediction of fatigue life and fatigue

3

strength of structure will occur if no concerted effort is made to apply test loads and environments in a realistic manner.

Further, the fatigue strength evaluation of a vehicle, whether by analysis or by test, should be made early in its design and fabrication stage. With this approach, it is practical either to redesign or to reinforce marginal and suspect regions of a structure before reaching the production stage of the vehicle. Careful attention to design details, coupled with the use of the most advanced structure stress-analysis techniques, will reduce the probability and the frequency of occurrence of underdesigned and fatigue-critical areas.

When knowledge of the magnitude of loads, frequencies of loads, and effect of environments is uncertain, there is but one course to pursue. For man-rated vehicles and for vehicles in which the retrieval of equipment and data is mandatory, the "fail-safe" design philosophy should be used. In this philosophy, the necessary structural reinforcements and redundant members are incorporated into the design so that, should accidental rupture or fatigue cracking in structure take place, a safe rather than catastrophic fracture would occur.

An alternate design and analysis procedure for the evaluation of fatigue resistance of structure is termed the "safe-life" method. In this concept, reliability of the fatigue resistance of structure is assured through knowledge that the vehicle either will be retired or will have accomplished its mission long before the fatigue life of its parts has been reached. It is believed that the use of this design approach should be limited to very few cases and then only with extreme caution. In the fatigue design of primary load-carrying structure, the safe-life method is not recommended for use.

STATE OF THE ART

General

Before the mid-1930's, the design of flight vehicles was based solely on the maximum load a structure could experience once in its lifetime. The design guides used during this period fortunately and unknowingly proved to be reasonable fatigue design criteria. Few, if any, catastrophic failures of structure could be attributed directly to metal fatigue. However, progress in man's demand for vehicles possessing increased performance characteristics advanced rapidly during the 1940's, and in the majority of cases, the design concepts required material allowables not yet defined and stress analysis techniques not yet developed. Although development of materials lagged the requirements of the designer, new materials eventually were produced and more exacting structural analysis methods were developed which, by degrees, evolved into designs possessing increased efficiency.

However, a forced trend toward higher and higher working stresses soon occurred which resulted in decreased margins of safety. Ultimately, a rapid rise in the number of structural fatigue problems was experienced. During the past 20 years there has been a gradual recognition of the fatigue problem and, today, the design of structural members, and especially structural joints, is no longer based on one maximum load. Now flight vehicle structures are designed and analyzed for a satisfactory life under the many small, repeated, and dynamic loads they will be subjected to in service.

Within the past 25 years, industry has spent a tremendous amount of effort to avoid catastrophic fatigue failures. Efforts also have been directed toward the avoidance of fatigue cracking which incurs costly maintenance problems. References 1 to 21 present good evidence of the efforts and successes experienced in the field. It should be recognized, however, that this success came about through a great mass of experience with flight structure and through acceptance of the fact that fatigue could occur in flight vehicle structure.

Experience in Space Vehicle System Designs

Conversely, current service experience with launch vehicle and spacecraft structure is rather limited. Fortunately, this lack of experience has not affected the majority of static firings and launches made, since they have been successful. However, this past performance alone does not assure continued success for all subsequent flights. Concerted efforts to develop structural testing and analysis techniques are required to maintain a high degree of structural integrity for future designs. It may be an unfortunate position for those who have conjectured that fatigue of launch vehicle structure is no problem because of its relatively short operational life. The same conclusion erroneously may be deduced for long-time operational spacecraft with its infrequently and low stressed structure. With the advent of man-rated space vehicle systems, coupled with the realization of the vastly different and unexplored fatigue regimes, this problem becomes important; since the occurrence of structural fatigue in flight is certainly probable. Table I identifies various structural categories related to the newer fatigue modes that must now be considered. These are high load-high cycle and low load-low cycle regions for both extremely short- and long-time exposures.

At present, it is known that fatigue is dependent on time, environment, and load cycle; for these reasons alone, the probability of occurrence of fatigue in metals and structures should not be overlooked. This is particularly true for the present class of space vehicle designs. It would be suicidal to adopt any other philosophy.

Current Evaluation Methods

The usual practice has been to define the fatigue characteristics of metals or of structural components by subjecting test specimens of the structural elements to repeated or alternating loads. By this procedure, design data are obtained to evaluate the effect of these alternating loads on structures. However, such fatigue programs have not always been wholly satisfactory for obtaining estimates of probable structure life or for defining rates of non-linear accumulative damage to structures. One of the principal reasons

Table I

FATIGUE REGIMES RELATED TO FLIGHT VEHICLE STRUCTURES

Structure	Target Life	Magnitude of Repeated Loads	Frequency of Occurrence of Repeated Loads	Operational Experience	Effect of Natural Environment in Reducing Vehicle Fatigue Strength
Commercial Aircraft	Approx. 20 yr.	Medium	High	High	Low to medium
Military Aircraft	4-8 yr.	High	Medium	Medium to high	Medium to high
*Launch	min.	High to very high	Medium	Low	Low to medium
Spacecraft	1-10 yr.	Low to medium	Low	Nil	Low to unknown

*Reusable boosters not considered

for this is that load cycles in fatigue testing usually are applied regularly, whereas in practice, loads on structures fluctuate indiscriminately.

In the design of many planned flight vehicles, current and future, it is necessary first to define the response of structures to random alternations of stress. These stress alternations arise from a disordered distribution of loads which is realistically encountered within vibration, acoustic, and turbulent-atmosphere environments.

Analytic methods have been developed for calculating the approach of failure of a structure subjected to these complex environments. In theory, the method predicts the damage imposed under random loads from the damage observed and measured under discrete amplitude loading. Although this method has been tentatively accepted, additional experimental data are required to demonstrate that the behavior calculated for random cyclical loading agrees with the observed phenomenon. Notably, this lack of experimental proof exists for such characteristic structural properties as fatigue life and fatigue-crack progression.

In summary, fatigue strength evaluations for the structure of space vehicle systems rests principally on results determined from laboratory tests. Recognition of the increased importance of testing is evidenced by the large number of space vehicle system tests completed and planned. Figure 1 shows a typical trend in the number of design evaluations required by one manufacturer for launch vehicle structure.

It is mandatory that any testing procedure, to obtain the required information, be appropriately applied, controlled, and monitored. Otherwise, predictions of structural behavior will be invalid. There are many references concerning acceptable testing procedures which are well worth reviewing before any structural fatigue investigation (see References 9, 10, 11, 13, 22).

In addition, dynamic as well as static stress analyses are necessary supports to testing evaluations for the prediction of service life. Dynamic stress analyses are probably more essential than ever before, since the complex

TRENDS IN FATIGUE/VIBRATION TESTING OF FLIGHT VEHICLE STRUCTURE M-22519
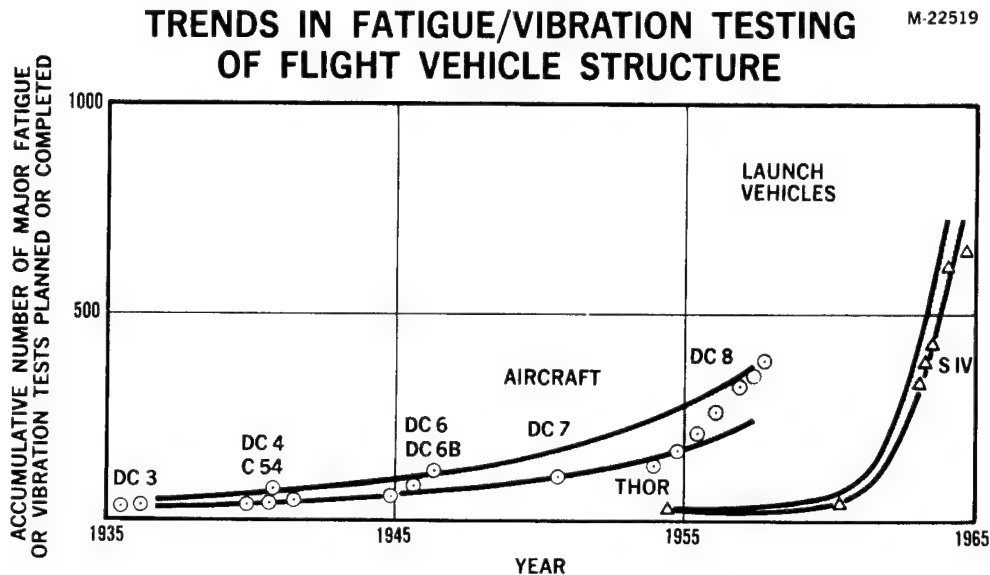
Figure 1

loads induced by vibration, acoustics, flutter, and buffeting are random in nature and all can contribute to the fatigue problem.

There is also a need for accumulative fatigue damage rules. It has been current practice to use the life-fraction concept (Reference 23) suggested by B.F. Langer in 1938. This theory suggested that if the fatigue life under a certain discrete load was N_1, and if n_1 cycles of this load were applied, then the fraction n_1/N_1 of the fatigue reserve of the structure was consumed. If this was followed by n_2 cycles of a load level corresponding to a life N_2 cycles, then an additional fraction n_2/N_2 was consumed. Failure, then, was predicted to occur when

$$D = \sum \frac{n}{N} = \frac{n}{N} + \frac{n_2}{N_2} + \frac{n_3}{N_3} + \quad \ldots \ldots = 1.0 \qquad (1)$$

In 1944, experiments were conducted at Douglas Aircraft Company which demonstrated this to be a reasonable rule (References 24, 25). Since these experiments, a number of investigations have been carried out and many

9

slight modifications have been suggested (see Appendix A). In 1956, A. K. Head and F. H. Hooke (Reference 26) suggested a cumulative fatigue damage rule for structure subjected to random noise.

By this rule, the life or number of cycles to failure for structure under random loading was calculated from the measured life under discrete loading and was expressed by the equation:

$$\frac{1}{N_R} = \sum \frac{x_i e^{\frac{-x^2}{2}} \Delta x}{N_{(x_i)}} \tag{2}$$

where

$\quad\quad x \quad\quad$ = ratio of peak stresses to the root mean square stress,

and

$\quad\quad N_{(x_i)} \quad$ = number of cycles to failure under discrete loading at each level of x.

This approach was used for structure having a single-degree-of-freedom response. In 1959, A. Eshleman (Reference 18) suggested equations for predicting the fatigue life and damage to structure having a two-degree-of-freedom response. In this method, the life under random loading was calculated from the following:

$$N_R = \left[\int_0^\infty \int_0^\infty \frac{P(x, y)\ dxdy}{Nxy} \right]^{-1} \tag{3}$$

where

$$P_{(x)} = x e^{\frac{-x^2}{2}} \quad, \quad P_{(y)} = Y e^{\frac{-Y^2}{2}} \quad \left(\begin{array}{l} \text{Rayleigh probability} \\ \text{distribution of} \\ \text{stress peaks} \end{array} \right)$$

and damage was predicted by

$$D = \sum \sum \frac{nxy}{Nxy} = 1.0 \tag{4}$$

It is believed that practical solutions to the fatigue problem for current space vehicle systems can be found by these methods. It is the intent of this report to outline procedures for analyzing, designing, and testing structure to satisfactorily withstand loads imposed during launch and space flight.

RECOMMENDED PRACTICES

Design Guides

At the present level of knowledge, it is impractical to quantitatively lay down the limiting fatigue design rules for specific structural configurations. The diversity in missions, loads, stresses, materials and environments certainly suggest this to be an impracticable, if not impossible, task. Qualitatively, however, the practices to be followed in the design of fatigue resistant structure can be defined, and if strict adherence to these established practices is carried out, then potential fatigue problems can be reduced in the initial stage of structural design.

Excellence in detail design, weight saving, and simplicity are all closely related. The result of these combined features is usually low cost, ease of fabrication, longer service life, and increased reliability, all of which are desirable characteristics. This is important from a practical point of view, since the scheduled design time allowed designers often is too short to develop and improve a complicated design. To the average designer a complex design may look better, more interesting, and more challenging, but it also can result in problems during test and in the operation of a vehicle. In general, the basic rules used in the airframe industry will apply in the design of space vehicle systems. Past experience and learning from the one field can be carried over to the other, although some precautions should be taken. Old designs may be unsuited to a new environment.

When procedures are proposed, they often become general rules which regulate structural design, even though they may be inappropriate. Recommendations used in the sense of "design guides" are far more appropriate. With this interpretation, a few of the more pertinent guides for the design of space vehicle systems may be listed:

(a) Keep the design simple.

(b) Provide for multiple load paths when feasible.

(c) Give extra consideration to tension loaded fittings and components.

(d) Apply fitting factors of safety to net stresses around holes and cutouts.

(e) Laboratory test all newly designed joints and compare with "time-tried" structures. (Figure 2)

(f) Utilize longitudinal grain direction of materials whenever possible (particularly for aluminum and steel alloys).

(g) Provide generous fillets and radii.

(h) Break all sharp edges - Polish critical regions if considered necessary.

(i) Reduce bearing stresses in riveted and bolted members to design minimums.

(j) Take precautions to protect parts from corrosion.

(k) Whenever possible reduce eccentricity of joints and fittings.

(l) Make doublers and structural reinforcements result in gradual, rather than abrupt, changes in cross-section.

(m) Provide easy access for service inspection of structure.

(n) Inspection procedures during fabrication and assembly of structure also should be provided.

(o) When practical produce parts and fittings from forged material rather than from extrusions or machined plate stock.

(p) Design parts for minimum mis-match on installation - this results in lower residual and preload tensile strains.

(q) Avoid superposition of "notches" in design.

(r) In some cases, when necessary, soft mount items that are critical for vibration environments.

(s) Select configurations with inherently high structural damping.

(t) Optimize bracket and component resonance frequencies considering both service environment and equipment fragility.

(u) Minimize the number of coupled resonances - that is, the number of vibrating components in series within a structural assembly.

(v) Stagger the resonances for the items within an assembly. (Mismatch impedances of mounted item and its bracket.)

(w) Make a proper selection of materials with cost, strength allowables, fabricability, and environmental effects in mind.

(x) Pay close attention to fabrication techniques for optimum forming of components.

(y) Establish reliable welding techniques for reproducibility of joint strengths.

(z) Construct rigid and precision tooling for the manufacturer of production parts.

Undoubtedly, there are additional fatigue design guides that are useful and could be added to the above list. Many such guides are unwritten and only intuitively known by the most experienced design specialists. Excellence in design, however, is not accomplished by the designer alone. It requires the close cooperation of specialists able to perform complex dynamic stress analyses, acousticians, vibration engineers, metallurgists, and specialists in structural testing and reliability analysis as well as those experienced in tooling and manufacturing. For example, many aerospace companies have initiated worthwhile training programs to inform their members of the fundamentals of the various disciplines. A designer cannot be expected to be an authority in acoustics or vibration, but a little knowledge in other fields can save considerable time and result in greater assurance of the success of the final design.

An example of the type of information available to the designer is shown in Figure 2. Although it may be difficult to accurately identify a new design on this chart, it does give a first approximation of life for typical construction if the working stresses are known. Another example of useful information for the designer is shown in Figure 3. The example shown is for bracket designs subjected to vibration environments. Many of these data are now available within the industry and could assist designers if the experiences of individual manufacturers were recorded on charts like that in Figure 3. Designer analysis of structure with the aid of this type of chart not only would save time in the production stress analysis but also would assure a higher probability of the structure passing the final qualification tests. A designer can be expected to have some knowledge concerning the calculations required for a dynamic stress analysis. These include the evaluation of such parameters as resonant frequency, impedance, and transfer functions for simple structure. But, the designer cannot be expected to be responsible for the final and formal dynamic stress analysis.

These guides and recommended training for designers are suggested for the sole purpose of reducing the overall development time from preliminary design lay-out to assembly in production.

AEROSPACE STRUCTURAL DESIGNS
(ALUMINUM ALLOY CONSTRUCTION)
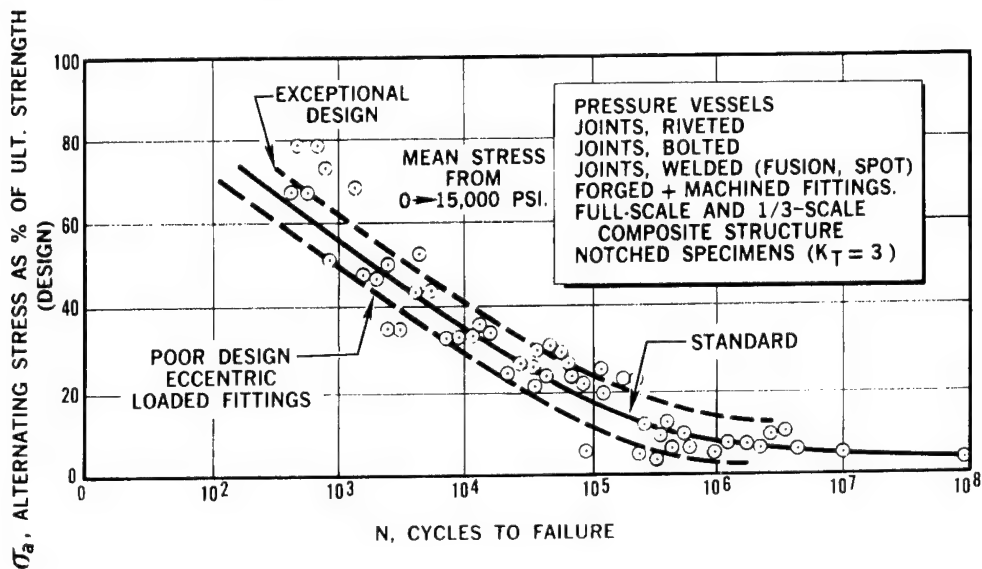
Figure 2

**EXPERIENCE IN
BRACKET DESIGN
VIBRATION
TESTING.***

*MEASURED DATA FROM
DEVELOPMENT/QUALIFICATION
TESTING:
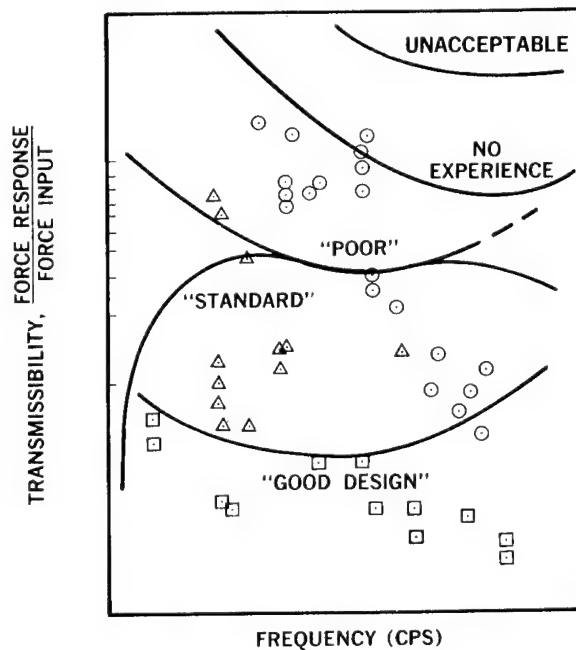
Figure 3

Testing Methods

This section briefly discusses various types of fatigue and vibration tests required in the evaluation of safe structure. Each type of test differs from the others and is performed for a specific purpose. The following major classes of fatigue test programs are used to evaluate structure:

(1) Experimental research
(2) Design development tests
(3) Qualification tests
(4) Production acceptance tests.

Experimental research. --Experimental fatigue research is carried out for the express purpose of defining the effects of various environmental parameters on the behavior of metals and structures. The laboratory specimens are usually simple elements and seldom possess the exact details of a functional design. The results of such investigations, however, are useful in design, but only qualitatively. Also, this type of testing can uncover other phenomena and direct further research. The appendixes at the end of this document suggest some areas in which further research is required.

Design development tests. --In the early stages of a design, it is good practice to perform tests on those structural arrangements that appear to be the most fatigue resistant. This type of test is not the final analysis of a design, but it often uncovers many undesirable structural characteristics. When this test technique is used, there is greater assurance that the design finally selected will be successful. If cost and excessive time do not allow this approach to be taken, the designer is then forced to rely upon past knowledge and experience.

In a fatigue test, it is desirable to evaluate as many replicate samples of a structural element as practicable. Accordingly, a design should be tested to the best estimate of the conditions that will occur under its planned and varying missions. The test loads imposed on a structure may be axial tension or compression, flexure, torsion, or combinations of these loads.

A specific test load should be applied in a realistic manner; under no circumstances should the fatigue characteristics of structure for one load type be assumed to be identical for an alternate load type. Similarily, the fatigue modes under sinusoidal wave loading should not be assumed to be identical with the failure modes under random loading. Techniques are available for the prediction of overall fatigue life under random loads from tests under constant amplitude loads, but considerable research is required to refine present methods of analysis. At the present time, no discrete load test can be considered to produce the equivalent damage of a random load test, although a close approximation of fatigue life under random loads can be made by the integration of damage incurred by a many-stepped discrete load spectrum. The procedures for making this numerical approximation are outlined in Appendix D.

In design development fatigue testing, the designer often encounters the problem of extrapolating experimental data. Normal experience has indicated that the final design loads for structure are different from the initial loads to which the early design was tested. However, this presents no serious problems. A common and acceptable method for extrapolating design data from a small amount of test data is illustrated by the following diagrams. This method will apply irrespective of the type of fatigue test or category of fatigue test data.

Figure 4 shows typical S-N curves for an example design problem. In the very early design stages, the fatigue characteristics were determined on inexpensive notched coupons representative of the design. A few more complex specimens of the final selected design were also tested. The fatigue lives of these test elements are not identical, but the characteristic shapes of the S-N curves can be assumed to be similar. With this technique, the results from a few tests can be extrapolated to define behavior over large ranges of loading conditions.

In this example, it is also assumed that the final design loads eventually were proven different from the initial test loads. It is not necessary to repeat the testing program, since it is possible to calculate the characteristics of the revised design environment from test results of the initial conditions. This

SN CURVE FOR COMPONENT X
EXTRAPOLATED FROM NOTCHED COUPON DATA.

M-22493

Figure 4

Legend:
- ○ NOTCHED COUPON, LH_2, R = .25
- □ NOTCHED COUPON, LN_2, R = .05
- ▲ COMPONENT X, LH_2, R = .26

$$R = \frac{MIN.\ STRESS}{MAX.\ STRESS}$$

Y-axis: MAX. STRESS – % OF ULTIMATE (80, 60, 40)

X-axis: CYCLES TO FAILURE (10^3, 5, 10^4, 5, 10^5, 5)

SN CURVE FOR COMPONENT X AT CONST. MEAN LOAD = 21% OF ULT.
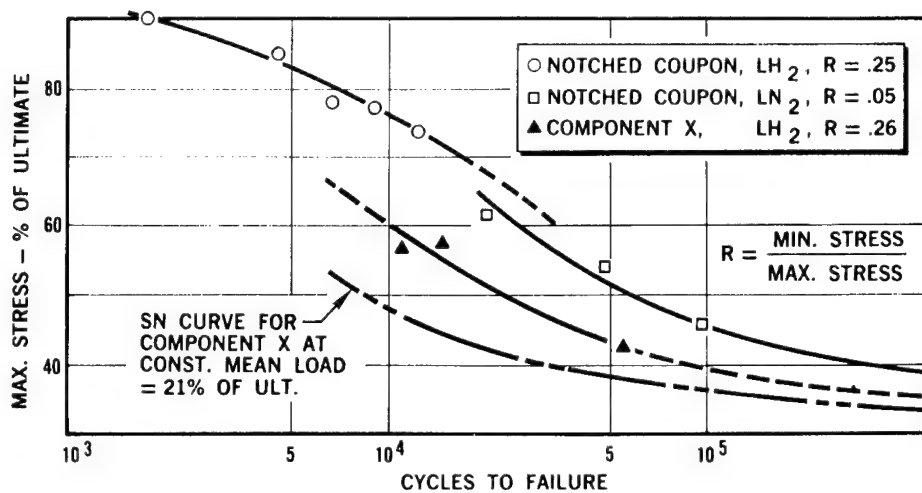
operation is performed with the aid of Figure 5. Extrapolated and inter-
polated values from the component S-N curve of Figure 4 are replotted in
Figure 5. Within reasonable limits, it is permissible to determine S-N
curves graphically for other stress ratios and stress ranges. In Figure 5,
a constant mean-load line equivalent to a load of 21% of the ultimate strength
of the component has been constructed. The maximum stress in a cycle and
the corresponding cycles to failure for this set of conditions can be read from
the figure and replotted as shown by the lower S-N curve in Figure 4.

Qualification tests. --It is current practice to evaluate the fatigue resistance
of space vehicle system structure by vibration and acoustic testing.
This type of test, referred to as a qualification test, is carried out on
test articles representative of production vehicle structure. In some cases,
tests are supplemented with analyses, although it is usual practice to perform
complex cumulative fatigue analysis only in those instances where failure oc-
curred during test. These safeguards are taken to prove the structural in-
tegrity of components, even though present qualification tests and their

19

M-22494

FATIGUE DIAGRAM
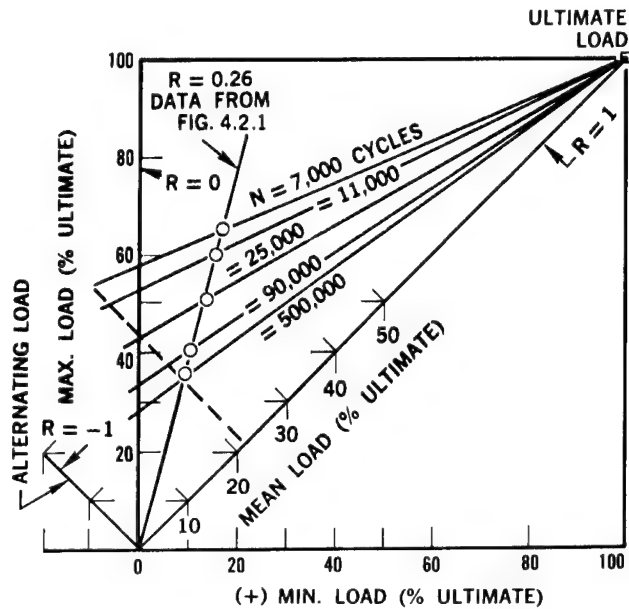
Figure 5

environments appear to be more severe than those encountered during actual vehicle operation. The severity of present test specifications suggests design penalties. However, until additional experience in the measurement of flight loads is gained, the test specifications should not be reduced. Table II illustrates some experience in the evaluation of fatigue in launch vehicle systems from their vibration, acoustic, and shock qualification tests. The number of test programs completed by one contractor is in the hundreds and the total number of programs planned exceeds a thousand. The number of test programs shown in the table represents only a small part of total industry experience. Nevertheless, it is believed that these few cases represent typical trends. Acceptance of the fact that fatigue could occur in launch vehicle structure prompted these design evaluations. This premise proved correct at least in the qualification testing phase, and increased numbers of design evaluations have been planned.

Table II

STRUCTURE QUALIFICATION TESTS

OCTOBER 1964

Program	Launch Vehicle A	Launch Vehicle B
Tests Planned	400	700
Total Number of Tests Completed	95%	25%
Number of Tests Passing Initial Test Program	20%	71%
Number of Tests Repeated (one or more times) Before Passing	80%	29%

Many of the initial Launch Vehicle A tests shown in Table II failed to pass the qualification program. Failure in many of these cases was attributed to fatigue cracking in a variety of components. When the preliminary test load criteria were released (References 33 and 34), they proved to be more severe than those to which the vehicle was originally designed. This situation was fundamentally responsible for requiring the redesign and retest of structural items. However, the experiences gained during this stage of development proved valuable, as evidenced by the increased number of Vehicle B components that passed qualification specifications.

Figure 6 shows a relatively large test article being readied for its vibration qualification test. The test article shown is the fuel line supported by the thrust structure of a large second-stage launch vehicle. It is mounted on an electrodynamic shaker which has a capacity of 32,000 lb. of force. The load and frequency spectrum for which this structure qualified is detailed in the test specification documents of References 33 and 34.

M-22531

VIBRATION QUALIFICATION
TEST FOR SIV THRUST
STRUCTURE AND
FUEL LINES
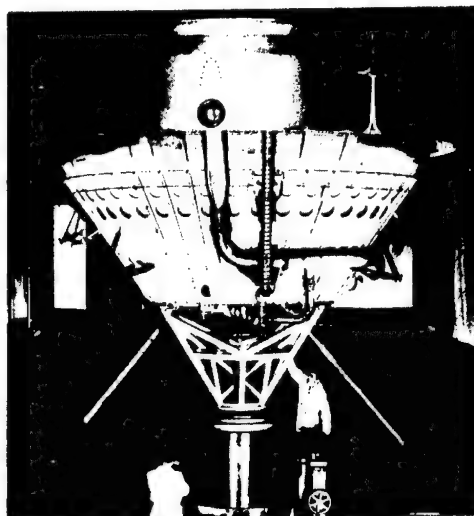
Figure 6

Production acceptance tests. --Acceptance testing of structure differs from
qualification testing in many respects. Acceptance tests are functional
tests in which the actual flight article undergoes various checkouts before
launch. Undoubtedly, the most damaging test phases are the fuel tank pres-
surization checks and the static firings. In qualification testing, the physical
and mechanical damage occurs in the structure of test articles that are later
discarded. However, in acceptance testing, fatigue damage is incurred in
the actual flight article and this is usually irreversible. Any amount of damage
generated in this manner accumulates with the damage produced during flight.
Since space vehicle systems must complete their missions without failure,
this makes knowledge of the fatigue characteristics of the structure and its
materials undergoing this type of test important.

In summary, four major types of test programs have been discussed. Each
serves a specific purpose. In many cases, all four types are required for a
given design. Further, it is necessary that the load and environment con-
ditions for a test be carefully simulated. The data collected from such tests

22

are usable in future designs. These data can provide knowledge and experience which the designer can use in the following ways:

(1) For the establishment of realistic test requirements.

(2) For the comparison of design and test requirements with actual conditions.

(3) For cumulative damage evaluations of structure. (The designer gains confidence when experiment equals theory.)

(4) For the estimation of vibration conditions on future flights.

Approach to Fatigue Life Prediction

The completion of three major tasks is required before the fatigue life of any structure can be evaluated. These tasks are as follows:

(1) Accurate definition of the loads and environments imposed on the structure.

(2) Calculations of structural response.

(3) Cumulative damage analysis and fatigue life prediction.

The complexity of the fatigue life prediction problem, as discussed in previous sections of this report, dictates that the technical disciplines of the stress analyst, dynamicist, acoustician, and metallurgist are all required for a solution to the problem. The interdependence of the three tasks above demands a coordinated effort within the various technologies to assure structural design free from premature fatigue failures.

Definition of load and environment. -- The sources and types of loads that may cause fatigue cracks or fatigue failure of structural and equipment components of space vehicle systems are itemized in Table III. Spacecraft structure can be affected by all loads experienced from the time of liftoff throughout the period of its flight mission, whereas the launch vehicle structure is affected only from liftoff throughout its atmospheric flight and to the instant of payload separation. Both types of structure are affected in varying amounts by prior handling and transportation loads.

Before a fatigue strength evaluation of a structural system can be performed, a quantitative definition of the shape, time of duration, and frequency of oc-

Table III

SPACE VEHICLE SYSTEMS = LAUNCH VEHICLE
STRUCTURE + SPACECRAFT

Load Source	Load Type	Cycle Load Wave Shape
Vehicle Transportation	Thrust-Buildup	Discrete
Pressurization	Shock	Sinusoidal
Engine Firing	Mechanical Vibration	Square
Atmosphere	Acoustic	Triangular
Stage Separation	Thermal	
Docking	Buffeting	Random
(Aerodynamic characteristics)	Gust and Wind Gradient	
Rotating Machinery (Centrifuge)	Maneuver	
	Residual (in fabrication)	

Load Duration	Load Frequency	Environment
Seconds	CPS	Corrosive
Minutes	CPM	Cryogenic
Hours Years	CPD	Elevated Temp.
		High Temp.
		Space Radiation
		Meteoroid
		Long-Time Vacuum
		Errosive (nozzles, pumps)

currence of the load cycles must be defined. In many instances, it will be necessary to include the effect of the appropriate environment acting in conjunction with the repeated dynamic loads for predictions of fatigue characteristics (see Appendix B).

At the present level of industry and government experience, there are two major classes of structural fatigue loading for which space vehicle components can be evaluated. These are as follows:

(1) The loads described by qualification test specifications.

(2) The loads based on the best estimate of loading within the prescribed vehicle mission profile, including loads inposed during acceptance testing.

The use of either Item 1 or 2 above in defining the dynamic structural response loads is dependent upon the degree of designer experience and the particular phase in design. In the preliminary design stage of a relatively new vehicle, it is not always feasible to evaluate reliably the structures environment or its dynamic loading in a quantitative manner. In these cases, it is recommended that structure be evaluated for a fatigue environment based on the loads prescribed by the qualification test specifications. In general, a fatigue analysis based upon these loads will provide a conservative estimate of the occurrence of failure and will result in a good overall reliability of the structural system. Principally, these loading specifications outline the magnitude and type of loads, the frequency spectrum, and the duration of the loads. Table IV describes a typical loading environment specified by the qualification test-loading spectrum. This testing environment can be designed to include the effects of all load sources and load types itemized in Table III. Figure 7 shows the various wave shapes associated with each loading.

In later design stages, instrumented vehicle flight data are often available so that the dynamic characteristics and induced loads may be better defined. This information can provide greater confidence that a proper selection in the loading history for future missions has been made. Eventually, qualification test specifications may either be modified or replaced with a realistic mission

Table IV

STRUCTURE QUALIFICATION TESTING
(Specifications Documented for Launch Vehicle Systems)

1.	Sinusoidal-Sweep	Rate and G level Specified
2.	Sinusoidal Resonance	Duration Specified for natural frequencies
3.	Random	Duration and power spectral densities (PSD) level specified
4.	Shock	Duration and peak G specified
5.	Acoustic	Duration and overall db -- level vs. frequency spectrum specified

M-22501

WAVE SHAPES-QUALIFICATION SPECS.

SINE SWEEP

SINE DWELL

RANDOM
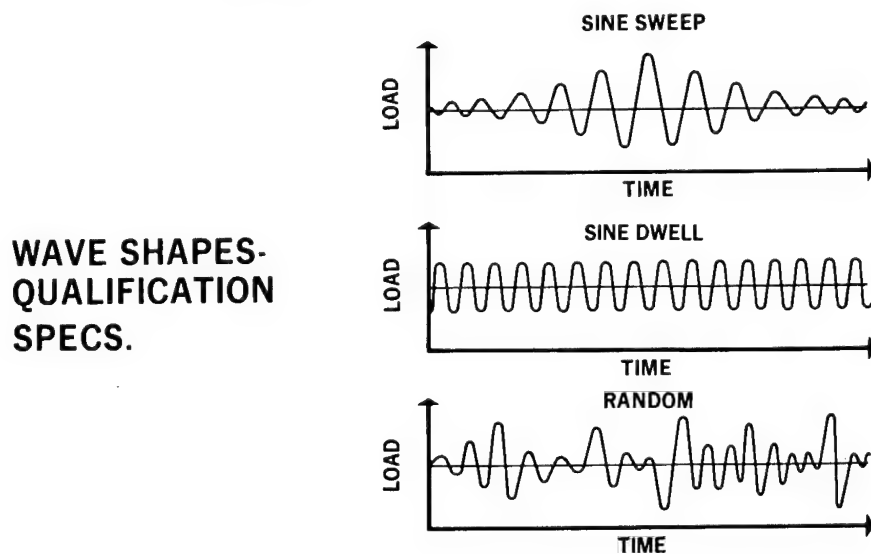
Figure 7

profile environment. Typical examples of recorded flight test data are plotted in Figures 8 and 9. From these data, histogram charts may be constructed for each phase of the prescribed mission as shown in Figure 10. Each block of the figure may include both discrete and random frequencies of loading in a narrow- or wide-band spectrum.

Prediction of structural response. --The problem of calculating the response of structure to a dynamic load environment begins by simulating the complex structure into an idealized system of lumped masses and springs capable of being analyzed by the dynamicist. By analysis methods, the mass matrix, damping matrix, and stiffness or influence coefficient matrix may be determined and the resulting transfer functions and natural frequencies of the structural system defined. Static analysis techniques are then used to determine the state of stress or load for the structural component for each of the resonant frequencies excited by the dynamic loading environment.

VIBRATION LEVELS MEASURED AT GIMBAL POINT IN S-IV-5 FLIGHT
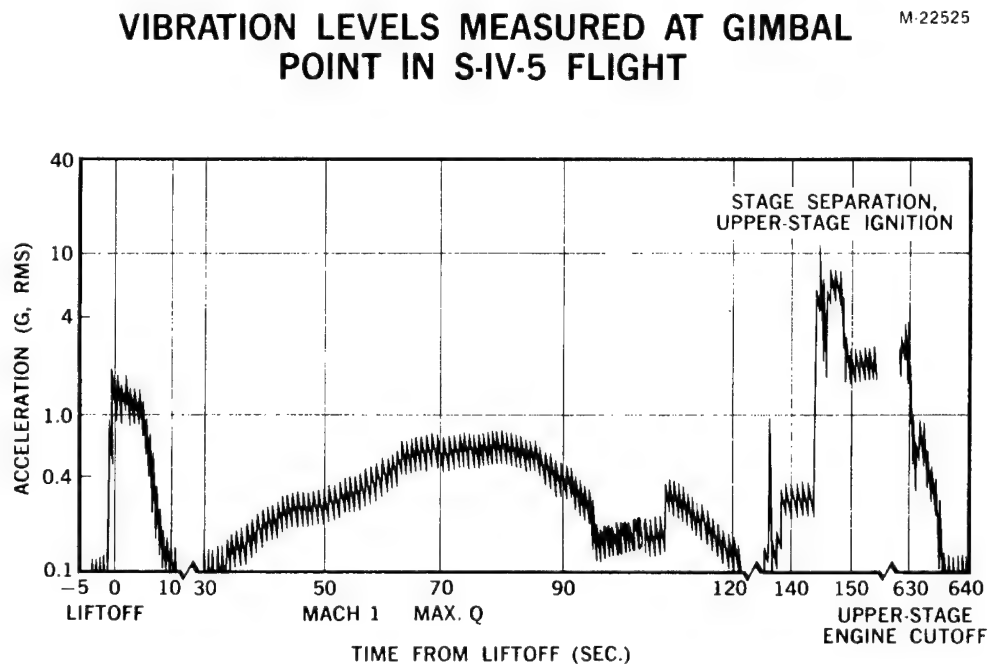
M-22525

Figure 8

VIBRATION LEVELS MEASURED AT GIMBAL POINT IN S IV-5 FLIGHT

M-22524
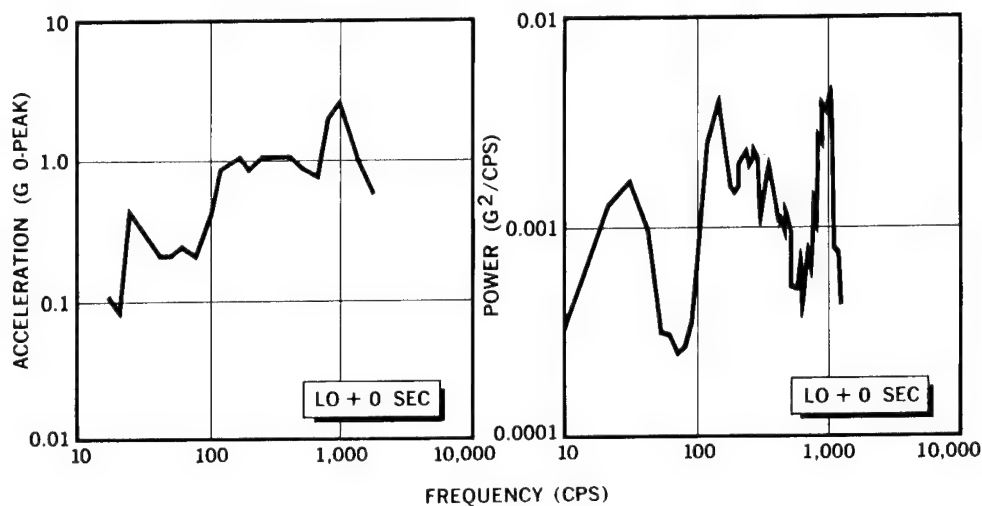
Figure 8 (cont)

EXTERNAL SOUND PRESSURE LEVELS MEASURED ON SI/SIV INTERSTAGE FLIGHT

M-22528
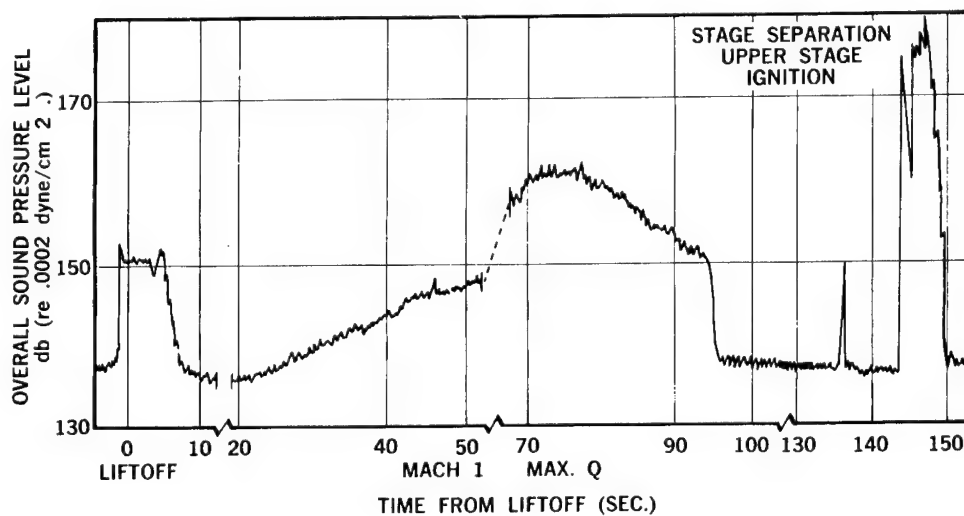
Figure 9

EXTERNAL SOUND PRESSURE LEVELS
MEASURED ON SI/SIV INTERSTAGE FLIGHT

M-22527

ONE-THIRD OCTAVE BAND LEVEL
db (re 0.0002 dynes/cm 2)

160

LO + 80 SEC.
OVERALL SOUND PRESSURE LEVEL

150

140

130

16 25 40 63 100 160 250 400 630 1,000 1,600

FREQUENCY (CPS)
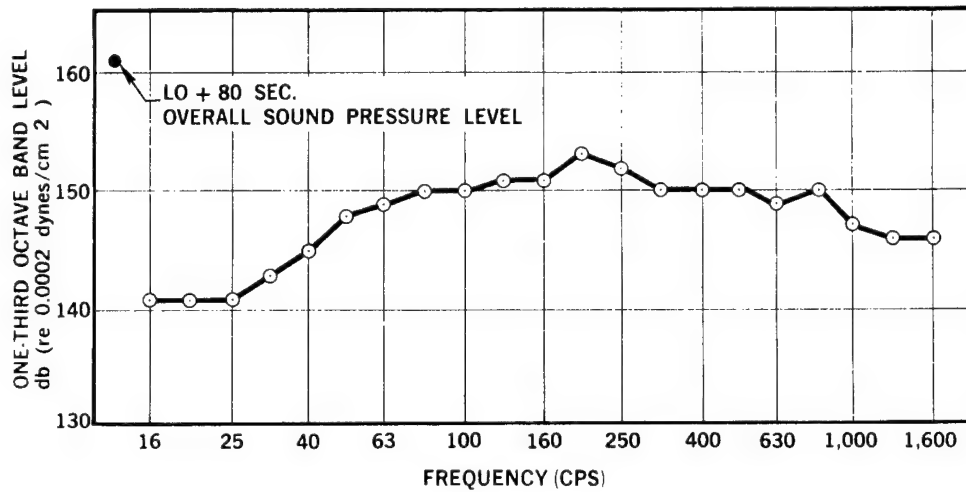
Figure 9 (cont)

EXAMPLE HISTOGRAM OF VIBRATION INPUT
TO "COMPONENT X" DURING EXPECTED LIFE

M-22508

LAUNCH VEHICLE + SPACECRAFT MISSION

OVERALL VIBRATION LEVELS (G RMS)

7
6
5
4
3
2
1
0

ACCEPTANCE
FIRING

476 SEC.

LIFTOFF

7 SEC.

POWERED
FLIGHT,
TRAN-
SONIC
MAX. Q

45 SEC.

STAGE FLIGHT

6 MIN.

AIR
TRANSPORTATION

TAKEOFF

4 MIN.

CLIMB

1 HR.

CRUISE

12 HR.

30 SEC.

SURFACE
TRANS.

135 MIN

1 MIN.

TIME

Figure 10

29
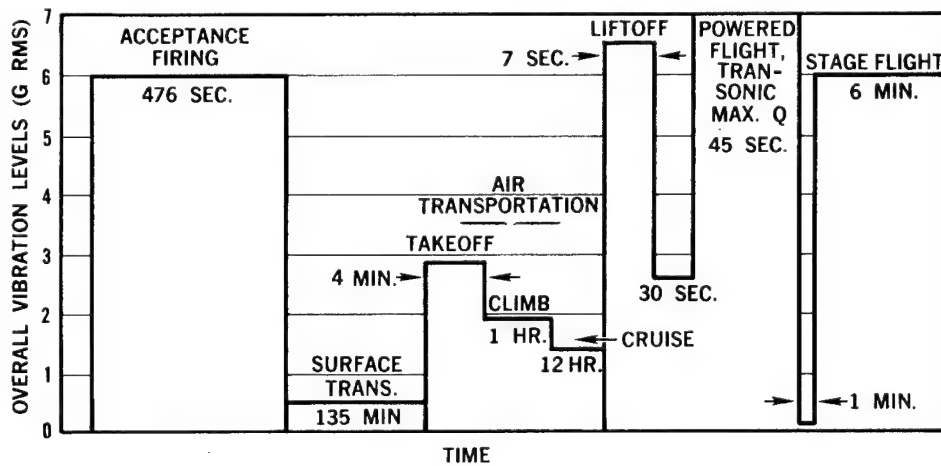
At this time, a cooperative effort between the structural designer and dynamicist is required to establish qualitative rules of design. The result is an improved design. For example, a design change in the structural stiffness could alter the natural frequency such that the resonance response loads are drastically reduced, or in some instances even eliminated. This change in the resonance frequency may be more advantageous from a weight consideration than a change in the strength characteristics.

Fatigue damage analysis. --With the dynamic loading enivronment defined and the response characteristics determined, the structure may now be evaluated for fatigue damage. Briefly, the problem is to determine the number of repeated load cycles for each of the wave shapes (i.e., discrete or random) and to assess the fatigue damage by using an accumulative damage technique. The fatigue damage is related to the S-N curve of the material or actual component. The S-N curves are determined through testing and characterize the cyclic load wave shapes and structural environment.

In the following section, a recommended analysis technique is used to describe a numerical example in detail. The example shown is for a component subjected to the mechanical vibration spectrum of a qualification test. The techniques used in the example can be applied to any loading analysis when the loads are random in nature. For an overall approach to a fatigue life prediction, the flow chart in Figure 11 is presented.

Fatigue analysis - example problem. --A recommended method for evaluating the fatigue life of a typical structural component subjected to mechanical vibration is described in detail in the procɜeding analysis. The limited scope of this section requires that assumptions be made in the analysis performed to characterize the static and dynamic behavior of the structural component. Briefly, these analyses require a structural idealization of the component in order to predict the static stress, the influence coefficients, and the modal response of the system.

FLOW CHART FOR FATIGUE LIFE PREDICTION

```
┌─────────────────────┐    ┌──────────────────┐    ┌──────────────────────┐
│ PRELIMINARY DESIGN  │    │ STRUCTURAL       │    │ DYNAMIC RESPONSE     │
│ (SIZING OF          │───▶│ IDEALIZATION     │───▶│ (NATURAL FREQ.       │
│ STRUCTURAL SYSTEM)  │    │ (INFLUENCE COEFF.)│   │ TRANSFER FUNCTION)   │
└─────────────────────┘    │ (MASS, DAMPING   │    └──────────────────────┘
                           │ AND STIFFNESS    │
┌─────────────────────┐    │ MATRIX)          │
│ MISSION  PROFILE    │    └──────────────────┘
└─────────────────────┘

┌─────────────────────┐    ┌──────────────────┐    ┌──────────────────────┐
│ PREDICTED LOADS     │───▶│ DYNAMIC LOADS    │◄───│ TEST LOADS           │
│ (HISTOGRAM)         │    └──────────────────┘    │ (QUALIFICATION       │
└─────────────────────┘                            │ SPECIFICATIONS)      │
                                                   └──────────────────────┘

┌─────────────────────┐                            ┌──────────────────────┐
│ S-N CURVES          │                            │ NUMBER OF            │
│ (MATERIAL OR        │           ┌────────────────┤ REPEATED             │
│ COMPONENT TESTS)    │           │ FATIGUE LIFE   │ LOAD CYCLES          │
└─────────────────────┘           │ PREDICTION     └──────────────────────┘
                                  └────────────────┘
```

Figure 11

For this example problem, it will be assumed that the qualification test spec-
ification has been selected as the critical vibrational loading for the component.
The qualification test specification used in this numerical example is shown in
Table V.   The sinusoidal-sweep loading is characterized by a continu-
ously varying excitation frequency, sweeping a broad band of frequencies at
a logarithmic rate. The sinusoidal-dwell loading, similarly referred to as
sinusoidal resonance loading, is limited to input frequencies at the major
resonant frequencies determined from the sine sweep tests. The random
vibration loading consists of a continuous distribution of amplitudes varying
in a statistical manner as a function of time. Investigation of the response
because of random loading requires the vibration to be described in spectral
terms. This is accomplished by subdividing the frequency band of interest,
measuring the mean square acceleration in each finite band and dividing by
the bandwidth. The function obtained when the bandwidths approach zero is
called the acceleration power spectral density (PSD - g^2/cps), and the plot
of PSD versus frequency is referred to as the power spectrum. Of the vibra-
tion inputs discussed, the random vibration more nearly duplicates the actual

31

Table V

QUALIFICATION TEST SPECIFICATION ASSUMED FOR
EXAMPLE PROBLEM - TWO AXES (X-Y)

Sinusoidal Sweep	5 to 50 cps at 0. 160 DA 50 to 2, 000 cps at 20. 4 g's at a logarthmic sweep rate of 1 min. per octave (sweeping up and back) for both axes (X-Y)
Resonance Dwell	5 to 50 cps at 0. 08 in. DA 50 to 2, 000 at 10 g's dwell 5 min. at each of the major resonances for each axis
Random Test	5 to 100 cps at psd from 0. 005 g^2/cps - 0. 50 g^2/cps 100 to 2, 000 cps at psd = 0. 50 g^2/cps 10 min. per axis

environmental condition experienced in most practical applications. Figure 7 shows the various wave shapes associated with the sinusoidal sweep, sinusoidal dwell, and random loads.

The input levels given in Table V are shown plotted in Figures 12 and 13. The double amplitude displacement in inches (DA) is expressed in terms of acceleration (g) by the following relationship:

$$g = \frac{\omega^2 (DA)}{386(2)}$$

where

ω = circular frequency ($2\pi f$)

simplifying results by substituting in the above equation

$g = 0.0511 \ f^2 \ (DA)$

32

SINUSOIDAL VIBRATION QUALIFICATION SPECIFICATION
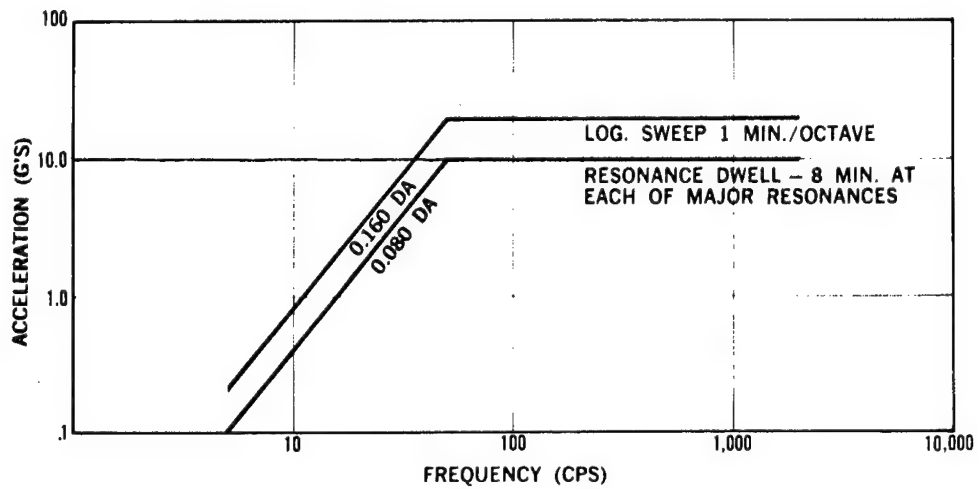
Figure 12

RANDOM VIBRATION QUALIFICATION SPECIFICATION
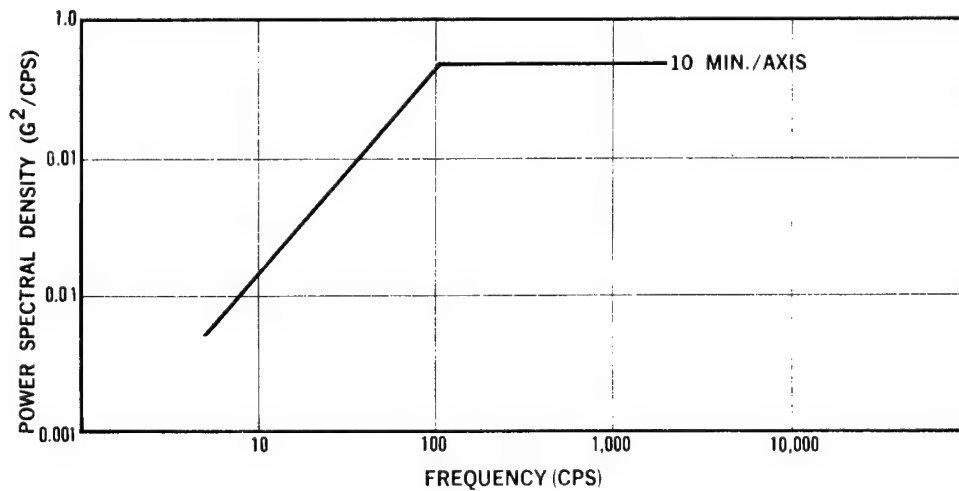
Figure 13

33

<u>Theoretical Response of Structural Component</u>:

From the static and dynamic analysis of the structural component, the
dynamic loads and transmissibility functions are assumed to have been deter-
mined for this example. Briefly, transmissibility functions are defined as the
ratios of the sinusoidal response of the component to its sinusoidal excitation
elsewhere, where both input and response are expressed in the same terms.
For the case of motion excitation, it is the ratio of the relative displacement
of the spring to the displacement of the foundation. That is

$$T_R = \frac{\delta s}{\delta F} = \frac{\text{Relative displacement of spring}}{\text{Displacement of foundation}}$$

For the structural component in this example problem, the transfer load func-
tions for a unit acceleration are depicted in Figure 14 for two axes of motion
(X, Y). By multiplying the qualification test input by the calculated
transfer load functions, the responses of the structural components are
determined.

M-22503

STEADY STATE TRANSFER FUNCTIONS
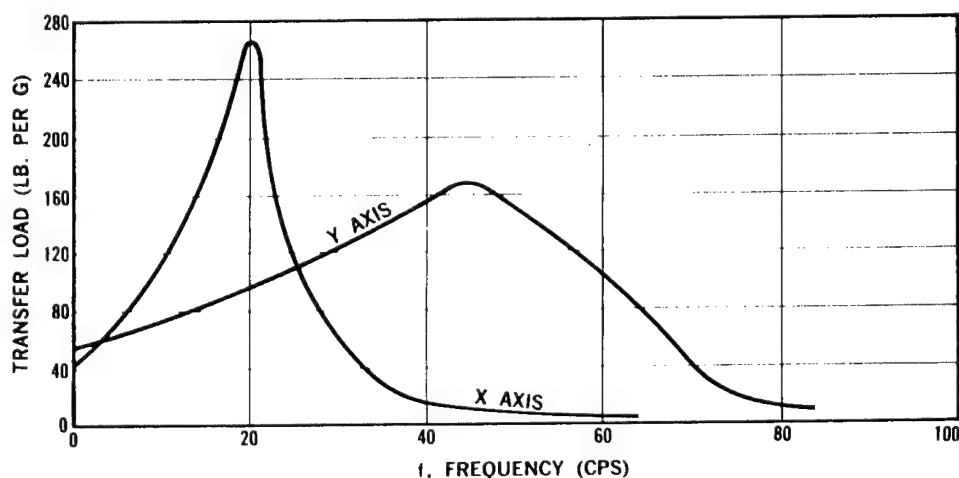
Figure 14

Sinusoidal-sweep and sinusoidal-dwell response--The theoretical transfer functions given in Figure 14 are multiplied by the qualification test inputs for the sinusoidal-sweep and sinusoidal-dwell conditions. These results are tabulated in Table IV and plotted in Figure 15.

Random response--The response to a random vibration input is obtained by multiplying the PSD's by the square of the transfer function; that is

$$R_{PSD} = PSD \times (TF)^2$$

where

PSD = Input power spectral density g^2/cps

TF = Transfer function lb/g

R_{PSD} = Response power spectral density lb^2/cps

The response power spectral density indicates the general level of vibration response only through a narrow frequency band. A more useful term in expressing random response is the root mean square rms value. By definition, the rms value is simply the square root of the area under the response power spectral density curve, where the abscissa is expressed in terms of frequency.

Although integration procedures may be used to evaluate the rms level of response for the example problem, considered in the analysis, the rms level may be approximated by the following equation

$$rms = \sqrt{\frac{\pi}{2} R_{PSD} \Delta f} \tag{6}$$

where

Δf is defined as the frequency band at the half power point (i.e., 0.707 $R_{PSD_{max.}}$).

The response power spectral density data for the two axes of motion are calculated in Table VII. These data are plotted in Figure 16. The computed rms levels are also indicated on this figure.

Table VI

f Frequency (cps)	Sweep g_s	Dwell g_D	Transfer Function- lb./g		Response Loads - lb.			
			S_x	S_Y	$S_x g_s$	$S_Y g_s$	$S_x g_D$	$S_Y g_D$
10	0.8	0.4	114	74	91	59	45	28
15	1.8	0.9	180	86	324	155	162	77
20	3.2	1.6	268	100	860	320	430	160
25	5.0	2.5	136	114	680	570	340	285
30	7.2	3.6	60	130	432	935	216	467
35	10.0	5.0	28	144	280	1,440	140	720
40	13.0	6.5	16	156	208	2,030	104	1,015
45	16.0	8.0	12	166	192	2,660	96	1,330
50	20.0	10.0	--	154	--	3,080	--	1,540
55	20.0	10.0	--	132	--	2,640	--	1,320
60	20.0	10.0	--	108	--	2,160	--	1,080
70	20.0	10.0	--	40	--	800	--	400
80	20.0	10.0	--	10	--	200	--	100
90	20.0	10.0	--	--	--	--	--	--

RESPONSE LOAD LEVELS FOR SINE SWEEP AND SINE DWELL
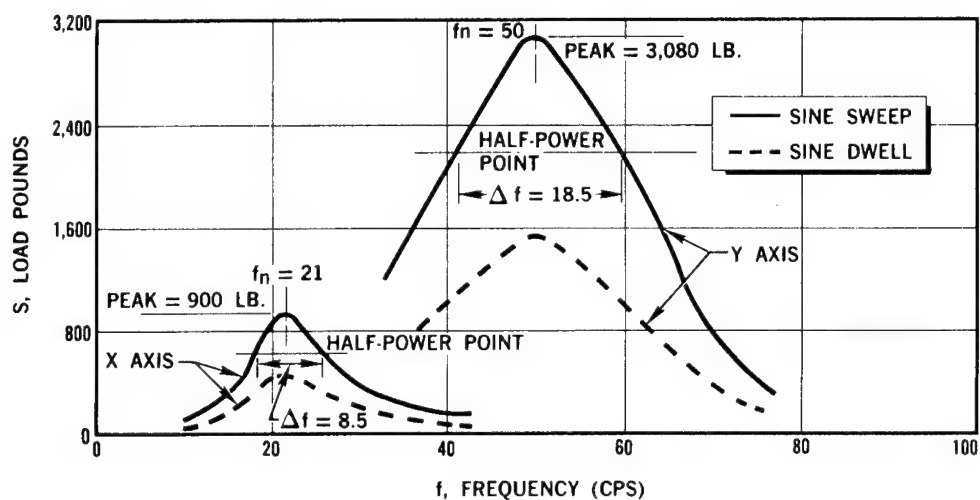
Figure 15

RANDOM RESPONSE LOAD LEVELS
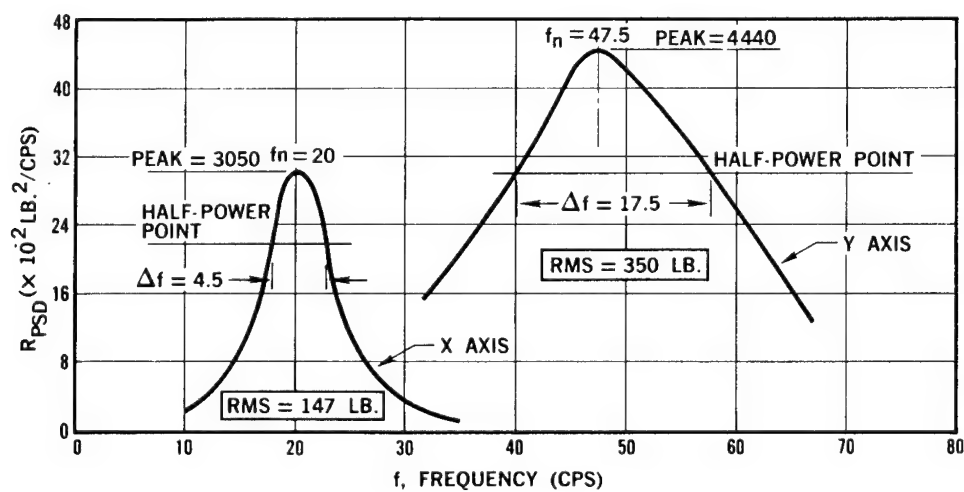
Figure 16

Table VII

CALCULATED RESPONSE POWER SPECTRAL DENSITIES

f cps	PSD g^2/cps	S_x lb./g	S_y lb./g	S_x^2 x10^{-3}	S_y^2 x10^{-3}	$(R_{PSD})x$ $= S_x^2$PSD	$(R_{PSD})y$ $= S_y^2$PSD
10	0.015	114	74	12.99	5.47	195	82
15	0.0275	180	86	32.40	7.39	891	203
20	0.0425	218	100	71.82	10.00	3,050	425
25	0.060	136	114	18.50	12.99	1,110	780
30	0.080	60	130	3.60	16.90	290	1,350
35	0.100	28	144	0.78	20.73	78	2,075
40	0.125	16	156	0.25	24.33	31	3,040
45	0.150	12	166	0.14	27.55	21	4,130
50	0.175	--	154	--	23.71	--	4,150
55	0.200	--	132	--	17.42	--	3,485
60	0.225	.	108		11.66		2,625
70	0.300		40		1.60		480
80	0.310		10		0.10		35
90	0.425		--		--		--
100	0.500		--		--		--
2,000	0.500						

$\downarrow$ $\downarrow$

Prediction of fatigue damage:

       Sinusoidal sweep--During the sinusoidal-sweep condition, the exciting frequencies are logarithmically sweeping through all of the component resonant frequencies and fatigue damage is incurred by each. However, the damage incurred sweeping through a major resonant frequency is great relative to other resonant frequencies, so that damage need only be evaluated for the major resonant frequency.

As the varying excitation frequency approaches or recedes from the resonant frequency, cycles of load occur that are less than the maximum and yet great enough to cause some fatigue damage. To evaluate this effect, only the response greater than the half-power points (i. e. , 0. 707 S_{max}) needs to be evaluated, since this level accounts for approximately 97% of the damage (Reference 22). The number of cycles, n, accumulated during a logarithmic sweep (up and back) between the half-power point at resonance may be expressed by the following relationship (Reference 38).

$$n = \frac{2T\ f_n}{\ln 2}\ \ln \frac{(f_n + 0.5\,\Delta f)}{(f_n - 0.5\,\Delta f)} \tag{7}$$

where

    T = Sec. /octave

    f_n = Major resonant frequency

    Δf = Bandwidth at resonance

The cycles accumulated by the structural component are calculated below. From the response load curves in Figure 15,

    Resonant frequency   = f_{n_x} =   21 cps

    Resonant frequency   = f_{n_y} =   50 cps

    Half-Power Point   =   0. 707 $S_{x_{max.}}$ =   647 lb.

    Half-Power Point   =   0. 707 $S_{y_{max.}}$ =   2,180 lb.

From the qualification specification input

$$T = 60 \text{ sec./octave}$$

Substituting for, n, results in

$$n_x = 1,570 \text{ cycles}$$

$$n_y = 3,340 \text{ cycles}$$

Assuming the accumulative damage theory, $\sum \frac{n}{N}$, adequate for this analysis, the total damage can be expressed as

$$D_{s_x} = \sum \frac{n_x}{N_x} \; ; \quad D_{s_y} = \sum \frac{n_y}{N_y} \tag{8}$$

where

N_x, N_y = Allowable number of fatigue cycles from the appropriate S-N curves for the structural component.

   Sinusoidal dwell--The calculation of the fatigue damage because of a sinusoidal-dwell condition is the simplest of the various vibration environments. Since the input loads are confined to the major resonant frequencies for a specified time, the total number of cycles may be computed from the following relationship

$$n = t f_n \tag{9}$$

where

   t = Time at major resonant frequency (sec.)

   f_n = Resonant frequency (cps)

From the response curve for the structural component shown in Figure 15, the number of cycles accumulated for each axis of motion is calculated.

From the curve

$$f_{n_x} = 21 \text{ cps}$$

$$f_{n_y} = 50 \text{ cps}$$

and

$$t_x = t_y = 5 \times 60 = 300 \text{ sec.}$$

substituting these values into the relationship $(n = t_{f_n})$ results in

$$n_x = 6,300 \text{ cycles}$$

$$n_y = 15,000 \text{ cycles}$$

the accumulated damage is expressed as

$$D_{d_x} = \sum \frac{n_x}{N_x} \;;\quad D_{d_y} = \sum \frac{n_y}{N_y} \tag{10}$$

Random test--Because the fatigue damage for the random loading occurs at each resonance frequency for the full duration of the specified environment, the probability of occurrence of resonant peaks is characterized from a statistical approach, where the damaging potential is related to the rms response.

The number of cycles, n, occurring during the random-loading environment is conservatively estimated to be

$$n = t f_n \tag{11}$$

where

t = total duration of loading

f_n = calculated resonant frequency

41

From the predicted and calculated response curve shown in Figure 16, the number of load cycles for each axis of motion of the structural component is calculated

where

$$t_x = t_y = 10 \times 60 = 600 \text{ sec.}$$

$$f_{n_x} = 20 \text{ cps}$$

$$f_{n_y} = 47.5 \text{ cps}$$

This results in

$$n_x = 12,000 \text{ cycles}$$

$$n_y = 28,500 \text{ cycles}$$

The accumulated fatigue damage is given as

$$D_{r_x} = \sum \frac{n_x}{N_x} \; ; \quad D_{r_y} = \sum \frac{n_y}{N_y} \tag{12}$$

The total fatigue damage for the three cyclic loading conditions of vibration is assessed by accumulating the damage associated with each. That is

$$D_x = D_{s_x} + D_{d_x} + D_{r_x} \tag{13}$$

$$D_y = D_{s_y} + D_{d_y} + D_{r_y} \tag{14}$$

Assuming that the appropriate S-N curves have been generated for the cyclic conditions of sinusoidal sweep, sinusoidal dwell and random loads, accounting for such parameters as stress concentration, stress ratios, and temperature, the fatigue life of the structural component in the example problem can be evaluated. It is well known, however, that little or no test data exist to develop S-N curves based upon varying load intensities such as the sinusoidal

sweep and random vibrational loadings. For convenience, laboratory tests on fatigue coupons are normally conducted under repeated loads with discrete stress levels and stress ranges. The reason is apparent when one considers the difficulty and cost in conducting coupon tests using nondiscrete loadings.

A recommended analytical technique for establishing S-N curves for the sweep and random vibrational loading based upon an equivalency with the standard, constant amplitude S-N test data is described in the following section. The analytical technique is based upon the method developed in References 22 and 39.

Equivalent S-N curves:

Sinusoidal sweep--As discussed previously, the damage suffered by sweeping through a major resonant frequency, compared with other resonant frequencies, is assessed only for the load level exceeding the half-power point. The predicted damage, sweeping through the defined bandwidth, is evaluated by dividing the bandwidth into ten equal intervals and summing the damage associated with each load level, based upon the constant amplitude S-N curve. This technique is described in detail in the proceeding analyses. Assuming a parabolic response curve for the sinusoidal loading, as shown in Figure 17, the damage is evaluated for the loads exceeding the half-power point,

where

$$P_1 = 0.997 \, P_a$$

$$P_2 = 0.974 \, P_a$$

$$P_3 = 0.927 \, P_a$$

$$P_4 = 0.857 \, P_a$$

$$P_5 = 0.763 \, P_a$$

PARABOLIC RESPONSE CURVE FOR
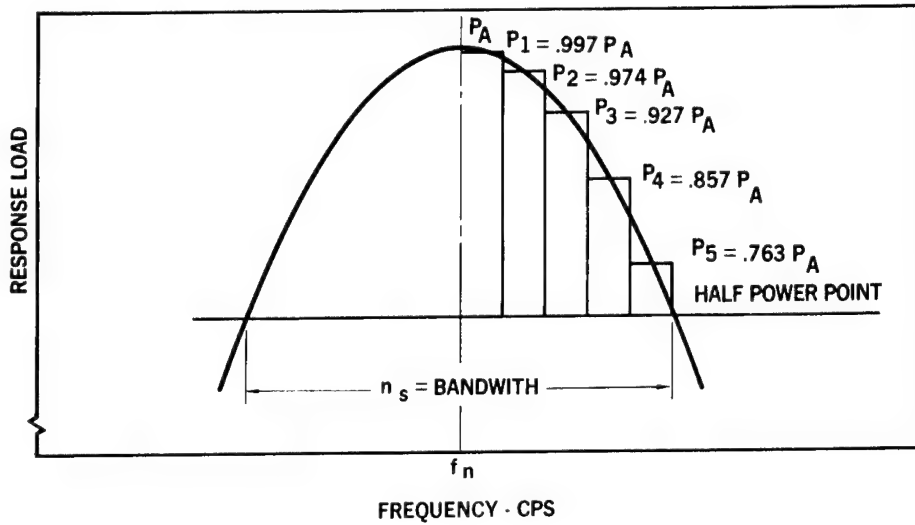## SINE SWEEP DAMAGE SIMULATION

Figure 17

The damage resulting from a major resonant sweep is given by

$$D_s = \frac{n_s}{N_s} = \sum_{i=1}^{5} \frac{n_s/5}{N(P_i)} = \frac{n_s}{5} \sum_{i=1}^{5} \frac{1}{N(P_i)} \tag{15}$$

where

$N(P_i)$ is defined by the constant amplitude load S-N curve.

Letting

$$N_i = N(P_i)$$

$$N_s = 5 \left[\sum_{i=1}^{5} \frac{1}{N(P_i)} \right] \tag{16}$$

44

Assuming that an appropriate constant amplitude (dwell) S-N curve defining
the material characteristics of the example structural component is established,
the equation is evaluated as shown in Table VIII. The calculated dwell S-N
curve and the tabulated results from Table VIII are shown in Figure 20.

Random S-N curves--Since the response of a single degree of freedom
system to random vibration is described as a random sine wave, the proba-
bility of peak loads or stresses within a narrow frequency band can be predicted
closely by a Rayleigh probability density distribution. The damaging potential
of the random vibration response, as discussed previously, is related to the
rms value.

The probability of peak response from the Rayleigh equation is given as

$$P(x) = x\,e\,\frac{-x^2}{2}$$

where   (17)

$$X = \frac{\text{Peak Load}}{\text{rms Load}}$$

Table VIII

EQUIVALENT SINUSOIDAL-SWEEP S-N DATA

P_a	P_1	P_2	P_3	P_4	P_5	N_1 $\times 10^{-3}$	N_2 $\times 10^{-3}$	N_3 $\times 10^{-3}$	N_4 $\times 10^{-3}$	N_5 $\times 10^{-3}$	N_s $\times 10^{-3}$
800	789	779	742	686	610	260	280	320	430	800	350
1,600	1,595	1,558	1,483	1,371	1,221	29	31	34	41	57	36
2,200	2,193	2,142	2,039	1,885	1,678	15	16	18	20	25	18
4,000	3,988	3,896	3,708	3,428	3,052	4	5	6	7	8	5

This probability density equation is plotted in Figure 18.

The evaluation of the probability of occurrence for $(X_o \leq X \leq X_o + \Delta X)$ is then defined as

$$\frac{n_x}{n_r} = \int_{X_o}^{X_o + \Delta X} P(x)\, dx \tag{18}$$

where n_r is the total number of random occurrences.

The above equation is evaluated and plotted in Figure 19. From the figure, the probability of the peak load exceeding the rms load is 60.65%, whereas the probability of the peak load > 2 rms is approximately 13%.

Because the occurrence of peak loads in a random process is statistical in nature and related to the rms load, fatigue damage can be calculated from the following equation

$$D_r = \frac{n_r}{N_r} = n_r \int_{o}^{\infty} \frac{P(x)\, dx}{N(x)} \tag{19}$$

In terms of the equivalent random cycles (N_r), the equation is expressed as

$$N_r = \left[\int_{o}^{\infty} \frac{P(x)\, dx}{N(x)} \right]^{-1} \tag{20}$$

or

$$N_r = \left[\int_{o}^{\infty} \frac{xe^{\frac{-x^2}{2}}\, dx}{N(x)} \right]^{-1} \tag{21}$$

RAYLEIGH DENSITY DISTRIBUTION OF PEAK RESPONSES FOR RANDOM VIBRATIONS
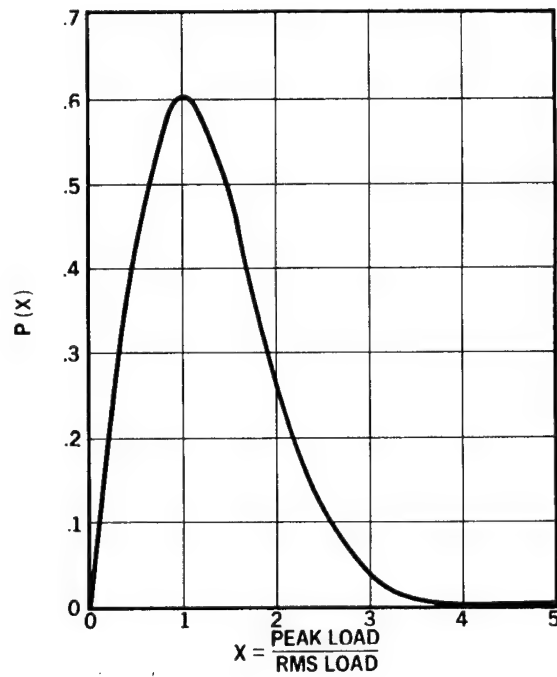
M-22485

$$X = \frac{\text{PEAK LOAD}}{\text{RMS LOAD}}$$

Figure 18

RAYLEIGH PROBABILITY OF PEAK LOADS EXCEEDING THE RMS VALUE

M-22506
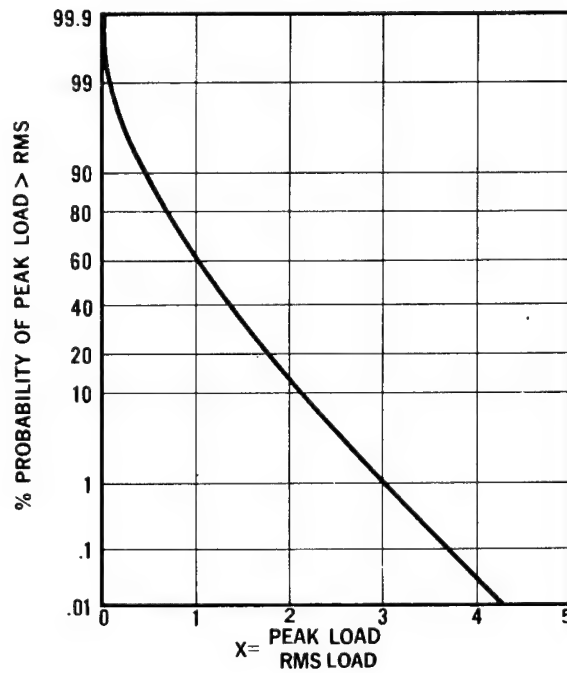

$$X = \frac{\text{PEAK LOAD}}{\text{RMS LOAD}}$$

Figure 19

47

The above equation is numerically integrated in Table IX for one point on the random S-N curve by assuming that

$$N_r = \left[\sum \frac{xe^{-\frac{x^2}{2}} \Delta x}{N(x)} \right]^{-1} \tag{22}$$

where

N (x) is defined by the dwell S-N curve for the structural component as given in Figure 20.

Other points were calculated to establish the S-N curve shown in Figure 20, but they are not tabulated in the table.

Table IX
EXAMPLE CALCULATION OF RANDOM S-N CURVE -
(RMS LOAD = 800 lb.)

X	$xe^{-\frac{x^2}{2}}$	Peak Load (lb.)	N (x) $\times 10^{-5}$	$\frac{xe^{-\frac{x^2}{2}}}{N(x)}$ (10^7)	x	$xe^{-\frac{x^2}{2}}$	Peak Load (lb.)	N (x) $\times 10^{-5}$	$\frac{xe^{-\frac{x^2}{2}}}{N(x)}$ (10^7)
0.60	0.501	480	20.00	3	2.4	0.135	1,920	0.19	71
0.80	0.581	640	5.40	11	2.6	0.089	2,080	0.16	55
1.00	0.606	800	2.60	23	2.8	0.054	2,240	0.14	38
1.20	0.584	960	1.30	45	3.0	0.033	2,400	0.12	27
1.40	0.525	1,120	0.76	69	3.2	0.019	2,560	0.11	17
1.60	0.445	1,280	0.48	93	3.4	0.010	2,720	0.09	11
1.80	0.356	1,440	0.36	99	3.6	0.005	2,880	0.08	6
2.0	0.271	1,600	0.28	97					
2.2	0.196	1,760	0.23	85					

$$N_R = \cfrac{1}{\Delta x \sum \cfrac{xe^{\frac{-x^2}{2}}}{N(x)}} = 6.66 \times 10^4 \; ; \quad \sum = 750 \times 10^{-7}$$

M-22507
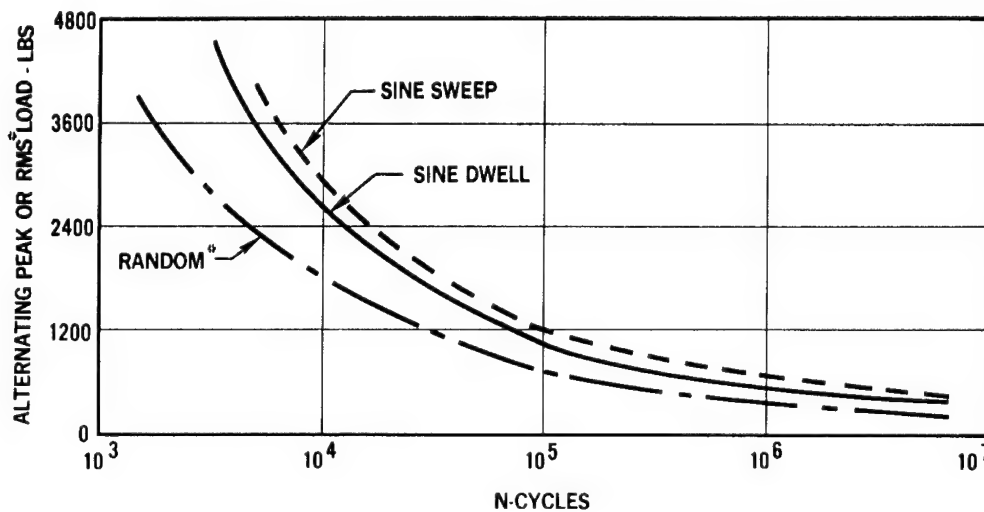
S-N CURVES FOR EXAMPLE COMPONENT

Figure 20

Fatigue life:

The fatigue life of the structural component may now be predicted by combining the appropriate damage equations. It was shown that the total damage for the two axes of motion may be expressed as

$$D_x = D_{s_x} + D_{D_x} + D_{R_x} \tag{23}$$

and

$$D_y = D_{s_y} + D_{D_y} + D_{R_y} \tag{24}$$

49

The assessed constant amplitude load (dwell) S-N curve in Figure 20 describes the material fatigue characteristics for one axis of motion. For two axes of motion, the fatigue characteristics may be different and may require two S-N curves to represent the material's fatigue life (see Appendix G).

For this numerical problem, the simplifying assumption is made that the depicted S-N curve is adequate for both axes of motion and that the total accumulated damage for the structural component may be expressed as

$$D \; = \; D_x \; + \; D_y \tag{25}$$

or

$$D \; = \; D_{sx} \; + \; D_{sy} \; + \; D_{Dx} \; + \; D_{Dy} \; + \; D_{Rx} \; + \; D_{Ry} \tag{26}$$

The damage equations are most conveniently used to evaluate the fatigue life of a structural component by presenting the results in the form of a life-block curve,

where

$$\text{life block} \; = \; \frac{1}{D}$$

One life block may be defined as one completed qualification test specification history on the component. To show satisfactory fatigue life, the component must withstand a minimum of one life block under these conditions without experiencing fatigue failure. A sketch of this curve is depicted in Figure 21.

The calculated life blocks for the structural component is tabulated in Table X from previously reported results. Additional calculations are made for loads both greater than and less than the original qualification test loading.
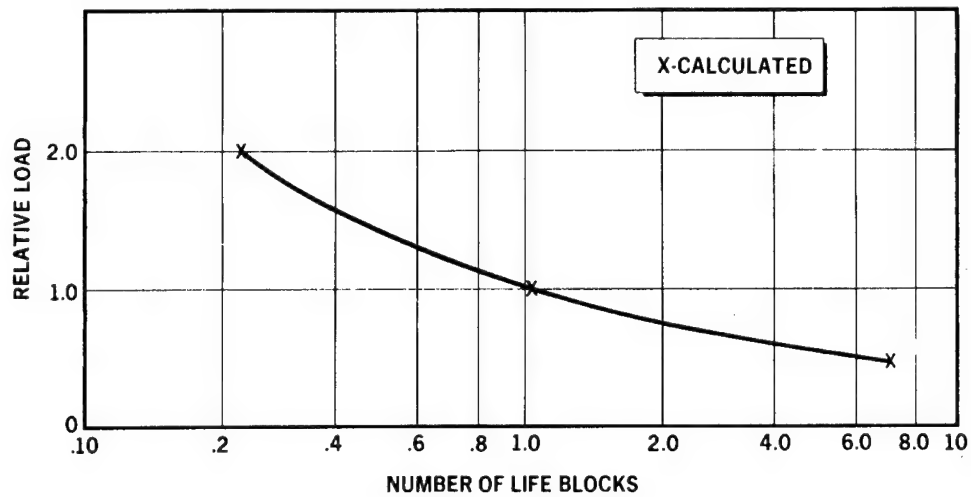
RELATIVE LOAD VS NO. OF LIFE BLOCKS
(EXAMPLE PROBLEM)

M-22488

Figure 21

Table X

COMPUTATION OF FATIGUE LIFE BLOCKS

Vibration		Relative Load = 1.0				Relative Load = 0.50			Relative Load = 2.0		
		n Cycles	Ref. Load lb.	N	$\frac{n}{N}$	Ref. Load lb.	N	$\frac{n}{N}$	Ref. Load lb.	N	$\frac{n}{N}$
Sweep	D_{sx}	1,570	880	2.5×10^5	0.006	440	5.0×10^6	≈ 0	1,760	2.3×10^4	0.063
	D_{sy}	3,340	3,080	9×10^3	0.371	15 to 40	4.0×10^4	0.083	6,160	1.6×10^3	2.090
Dwell	D_{Dx}	6,300	440	2.2×10^6	0.003	220	∞	0	880	1.5×10^5	0.042
	D_{Dy}	15,000	1,540	3.2×10^4	0.470	770	3.0×10^5	0.050	3,080	7.2×10^3	2.083
Random	D_{Rx}	12,000	147	∞	0	104	∞	0	208	6×10^6	0.002
	D_{Ry}	28,400	350	9×10^5	0.032	246	4×10^6	0.007	490	2.6×10^5	0.119
Damage		$D_1 = \sum 0.882$				$D_2 = \sum 0.140$			$D_3 = \sum 4.404$		
Life Blocks		$\frac{1}{D_1} = 1.134$				$\frac{1}{D_2} = 7.150$			$\frac{1}{D_3} = 0.227$		

CONCLUSIONS

Initial fatigue design guides for space vehicle structures, based on actual design experiences, are summarized in the following list:

1. Launch vehicle structure and spacecraft structure should be examined in the early design stage to determine the probability of the occurrence of structural fatigue.

2. Full-scale test articles or components of space vehicle systems should be subjected to rigid qualification tests (see, for example, Reference 33). If such tests reveal marginal or suspect designs, an evaluation of the test results should be supplemented with analysis.

3. It should be shown by analysis that fatigue damage incurred during acceptance testing on full-scale or component parts of actual space vehicle systems will not adversely affect the success of a subsequent mission.

4. The space vehicle system flight article or its components must withstand, without failure, the load frequency intervals and load spectra to which it (or they) will be subjected during operation. At present, the structure appears to be more susceptible to fatigue during launch. Structure designed to withstand boost environments will, in all likelihood, be acceptable for the infrequent loading imposed by the space environment.

5. Under the operating conditions stated in Item 4, and with lightweight design as a goal, the present fail-safe (fracture-safe) design may have to be drastically altered for spacecraft structure. The tolerable flaw or crack sizes will have to be defined in the early design stage.

6. The simultaneous action of fatigue and the great range of space environments has varied effects on metals and structures. These effects must be considered in the design of structure. Although experience in the design of space vehicle systems is relatively limited, sufficient knowledge does exist to produce safe vehicles.

end

APPENDIX A

CUMULATIVE FATIGUE DAMAGE ANALYSIS FOR
LABORATORY SPECTRUM LOAD TESTS

The cumulative fatigue damage concept, $\sum \frac{n}{N}$, originally formulated suggested that damage accumulated at a linear rate. Since its conception, this has been proven false many times. It is now known that physical damage to structure by fatigue action progresses at an exponential rate similar to the rate of fatigue crack growth. Also the effects of prior history, such as the effects of intermittent high tensile or compressive loads, have been shown to greatly alter nominal fatigue lives.

Based on these observations, modifications have been made to the fatigue damage rule which are quite general. The method to be presented has been used in the fatigue analysis of spectrum loaded structure in the laboratory and has been quite successful.

The Mean Damage Rate Method (Reference 4)

A simple mathematical expression has been found whereby the value of $\sum n/N$ can be computed for spectrum loadings when certain conditions are met. These conditions are as follows:

1. The nonlinear damage curves are known as functions of the cycle ratio and the prior history.

2. The loading history is a periodic function of time. Within a period or block, the load levels assume a certain pattern which is repeated in each subsequent block.

3. The number of cycles per block is small compared to the total life.

Under these assumptions, the cumulative cycle ratio is given by

$$\sum \frac{n}{N} = \int^{X_{cm}} \frac{dx}{\overline{X}'(X)} \tag{1}$$

The derivation of this expression is given in Reference 4. The meanings of the symbols are most easily understood through reference to the damage

curves of Figure A1. Thus, X is the damage ratio, which can best be visualized as ℓ/w, where ℓ is crack length and w is specimen width. The cycle ratio u is equal to n/N. The critical damage ratio is X_c, equal to ℓ_c/W, where ℓ_c is the critical crack length. The symbol X_{cm} denotes the minimum critical damage ratio for all of the damage curves associated with the various load levels within the block. The prime denotes differentiation with respect to u, so the X_i' is the slope of the ith damage curve. The symbol $\overline{X}(X)$ denotes the weighted average slope of all the damage curves at any given value of X. The weighting is done according to the percentage of the block devoted to each load level. Thus,

$$\overline{X}'(X) = \sum_{i=1}^{m} X_i' r_i \qquad (2)$$

where r_i is the ratio of the number of cycle ratios at the ith load level to the total number of cycle ratios in the block.
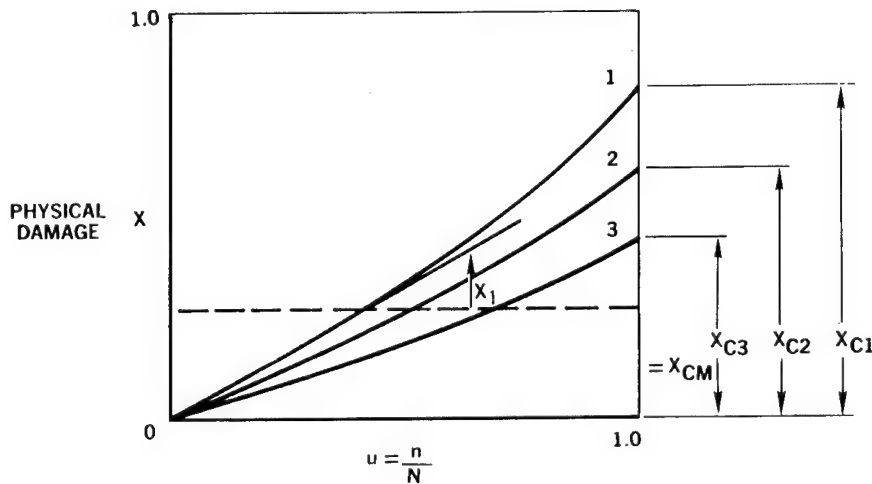
M-22511

DAMAGE CURVES

Figure A1

56

The integration indicated in Equation 1 can be performed graphically, numerically, or, when the damage curves are given by integrable mathematical expressions, directly. In Reference 4, this integration has been performed directly for curves corresponding to a modification of Henry's formula for damage propagation.

The formula corresponding to Henry's damage was used to calculate the value of $\sum n/N$ for vanishing block size for the same numerical values used in the digital computer calculation, presented in Figure 66 of Reference 4. The formula gives $\sum n/N = 0.730$, which agrees with the digital computation as $\Delta n \rightarrow 0$.

For continuous spectra, the summation of Equation 2 must be replaced by an integration as follows:

$$\bar{X}'\,(X) \;=\; \int_{-\infty}^{\infty} r\,(\sigma)\, X'\,(\sigma)\, d\sigma \tag{3}$$

where σ is an environmental parameter, and $r\,(\sigma)$ is a probability density distribution having the properties

$$r\,(\sigma) \gtrless 1 \text{ and } \int_{-\infty}^{\infty} r\,(\sigma)\, d\sigma \;=\; 1 \tag{4}$$

The limiting value of $\sum n/N$ for spectrum loadings, according to Henry's formula, can be obtained by substituting Equation (6) into the mean damage rate formula (Equation 1). This manipulation is performed in Appendix A of Reference 4. The result is summarized in Figure A2, which gives $\sum n/N$ as a function of the parameters involved. An example of the use of this figure follows.

If other formulas for damage propagation should turn out to be more suitable than Henry's, they can be substituted into Equation 1 to give new expressions for $\sum n/N$. Therefore, the mean damage rate formula is quite general.

$\Sigma \dfrac{n}{N}$ FOR SPECTRUM LOADINGS BASED ON HENRY'S EQUATION MODIFIED*

$$\alpha_0 = \sum_{i=1}^{m} \frac{r_i \, x_{ci}}{1 + k_i}$$

$$\alpha_1 = \sum_{i=1}^{m} \frac{r_i \, k_i}{1 + k_i}$$

$$\alpha_2 = \sum_{i=1}^{m} \frac{r_i \, k_i^2}{(1 + k_i) \, x_{cj}}$$

$$b_1 = \alpha_0 \alpha_2 - \alpha_1^2$$

$$b_2 = \frac{\alpha_0}{x_{cm}} + \alpha_1$$

LINEAR RULE

$$*\frac{x}{x_c} = \frac{u}{1 + k \, (1 - u)}$$

$$\Sigma \frac{n}{N} = \frac{1}{\sqrt{b_1}} \, \text{TAN}^{-1} \frac{\sqrt{b_1}}{b_2} \quad \text{WHEN } b_1 > 0$$

$$= \frac{1}{b_2} \quad \text{WHEN } b_1 = 0 \qquad = \frac{1}{2 \sqrt{-b_1}} \, \ln \frac{b_2 + \sqrt{-b_1}}{b_2 - \sqrt{-b_1}} \quad \text{WHEN } b_1 < 0$$

(Vertical axis: $\Sigma \frac{n}{N}$, values 0, 0.4, 0.8, 1.2, 1.6. Horizontal axis: b_1, values −1, 0, 2, 4, 6, 8, 10. Curves labeled 1.2, 1.0, 0.8, 0.5, 1.5, b_2.)
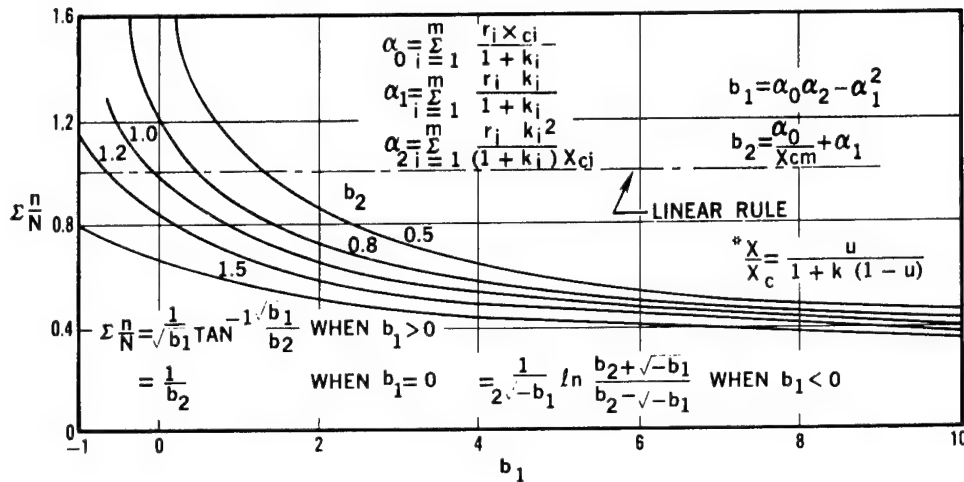
Figure A2

Example computation by mean damage rate method. --Given a spectrum con-
sisting of cycle blocks defined by the following table. The maximum stress,
the endurance limit, the number of cycles per block, the life, and the critical
crack length for each stress level are assumed to be known. The calculation
is carried out using Henry's constant as $K = E/(S-E)$.

HENRY'S EQUATION MODIFIED

Henry (Reference 27) has given the equation

$$D = \frac{n/N}{1 + K \, (1 - n/N)} \tag{5}$$

as the equation of the damage curve, where $K = E/(S-E)$, S = maximum stress,
and E = an endurance limit stress.

The following modification of Henry's formula is proposed for some applications:

$$\frac{D}{D_c} = \frac{n/N}{1+K (1-n/N)} \tag{6}$$

where D_c is the critical damage, which is the damage at which the part fractures completely. In Equation 5, the critical damage is unity. With Equation 6, the damage curves tend to have the character shown in Figure A1. The curves for high stress tend to have less curvature and a lower value of critical damage (critical crack length) than the curves for low stress.

Figure A3 shows the fatigue results of prior loaded laboratory specimens by both tension and compression prestrains. If the preload is tension and exceeds the maximum cycling load in the fatigue test, an improvement in life is observed. If the prior preload is compression, a reduction in overall life occurs. (See footnote in Table A1.)
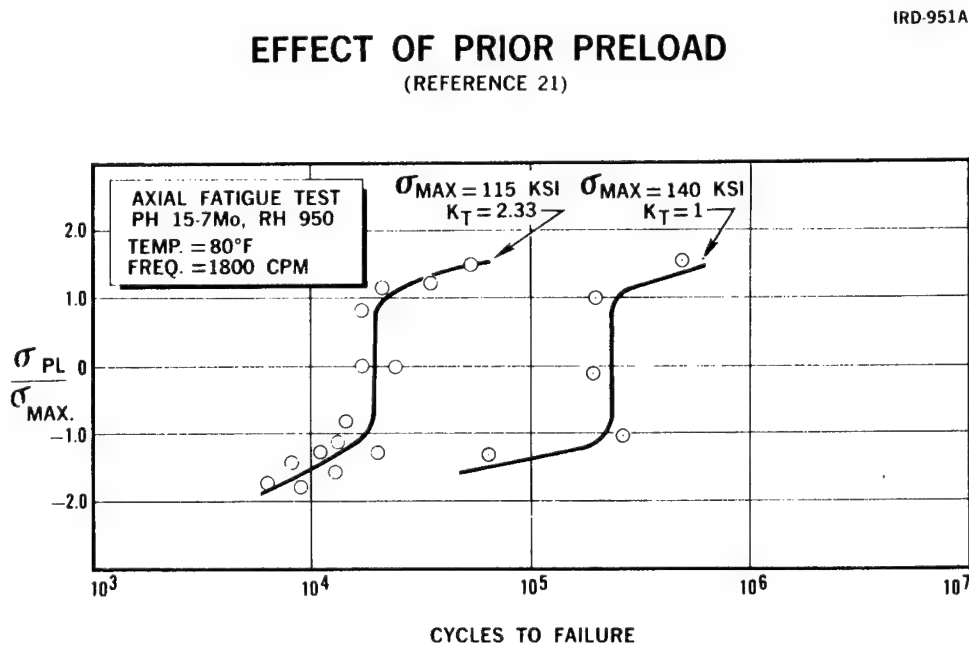
IRD-951A

EFFECT OF PRIOR PRELOAD
(REFERENCE 21)

Figure A3

Stress Level	Max. Stress S	End Limit E	Cycles $\overline{\text{Block}}$ δn	N* (cycles)	$K = \frac{E}{S-E}$	$\Delta u = \frac{\delta n}{N}$	$r = \frac{\Delta u}{b}$	Critical Crack L. X_c
1	117,800	110,000	160	9,000	14.1	0.01780	0.4826	0.388
2	132,100	110,000	40	4,200	4.98	0.00954	0.2588	0.345
3	146,400	110,000	8	2,800	3.02	0.00286	0.0775	0.308
4	165,900	110,000	1	2,200	1.970	0.00045	0.0122	0.263
5	138,200	135,000	32	8,500	42.2	0.00377	0.1022	0.443
6	152,500	135,000	8	5,000	7.71	0.00160	0.0434	0.397
7	166,800	135,000	3	3,500	4.25	0.00086	0.0233	0.355
						0.03688	1.0000	
						$(b = \sum \Delta u)$		

*If altered by preload effects, the discrete value of N may be obtained from ad-hoc tests as shown in Figure A3.

Stress Level	$\frac{r}{1+k}$	$\frac{k}{x}$	$\frac{rx}{1+k}$	$\frac{rk}{1+k}$	$\frac{rk^2}{(1+k)x}$
1	0.0320	36.4	0.01241	0.451	16.41
2	0.0433	14.41	0.01493	0.215	3.10
3	0.01925	9.80	0.00594	0.0582	0.570
4	0.00410	7.49	0.001080	0.00810	0.0606
5	0.001956	95.5	0.000866	0.0827	7.90
6	0.00497	19.42	0.001975	0.0384	0.746
7	0.00444	11.98	0.001578	0.01890	0.226
			0.0388 (a_o)	0.8723 (a_1)	29.013 (a_2)

$$b_1 = 0.0388 \times 29.0 - 0.872^2 = 0.365$$

$$b_2 = 0.0388/0.263 + 0.8723 = 1.020$$

$$\therefore \sum \frac{n}{N} = 0.890 \text{ (from Figure A2)}$$

APPENDIX B

ENVIRONMENTAL EFFECTS ON THE FATIGUE
STRENGTH OF STRUCTURE

Phenomena such as fatigue, creep, stress corrosion, embrittlement, and delayed fracture (static fatigue), acting alone or in combination, are all damaging to structural materials. The damaging effect of each of these environments on structure is not single-valued but will vary as often as the conditions of service are altered. This makes calculations for the prediction of environmental effects extremely difficult. Meaningful evaluations of the effects on structure can be made by careful simulation of the environment during tests. However, such simulation often is a difficult and costly approach to the solution of the problem. For this reason, accelerated test methods are constantly being sought. Historically, it can be shown that no accelerated test technique yet devised will accurately predict the "time" required to reach critical cracking or critical damage in structure. Concern for the damaging effect of fatigue in structure was reported as early as 1829. Since that time, a great amount of research and progress has been made. It is needless to itemize the successes and failures in controlling this phenomenon since they are well known. However, many failures in the predictions for behavior can probably be attributed to inadequate test evaluation methods, many of which are still in use today. For example, the use of high speed testing machines to evaluate fatigue resistance at elevated temperature and in oxidizing atmospheres will yield invalid data for parts designed for low strain rates.

It is not the purpose of this appendix to recommend acceptable analytic or test evaluation methods, nor is it the purpose to discuss their limitations. The purpose is to illustrate the effects of a variety of environments. The characteristic effects of many environments are not well known to the average structural designer, but this knowledge is both useful and necessary if safe structures are to be designed. The following discussions and illustrations define some of the more pertinent fatigue characteristics of metals and metal structures.

Figure B1 shows fatigue-crack growth characteristics as a function of environmental temperature. In this diagram, the stress range and stress level producing cracking are the same for all test temperatures noted. Several distinctive characteristics are evident in this figure. The diagram shows that the fatigue life increases as the temperature decreases. It also illustrates a reduction in the critical flaw size or crack length that can be tolerated as the temperature of a metal decreases. It also indicates that as the temperature decreases the crack nucleation period or time to produce an observable crack increases. Conversely, as temperature decreases, the period of observable fatigue crack growth decreases.

Figure B2 shows experimental results of a study of crack growth under steady-state loading conditions and at elevated temperatures. In these tests, fatigue cracks were grown in 6-in.-wide aluminum panels. The panels were then held under constant loads and temperatures. Within a few hours, creep cracking had advanced to a critical stage. Although the temperature level used in the experiments was higher than the useful temperature of the material, it should be realized that the same phenomenon could occur around 200°F (solar radiation) and probably in fewer than 10,000 hours (long-operational spacecraft).

Figures B3 and B4 show fatigue test results as dependent on test temperature. In these illustrations the total number of cycles-to-rupture as a function of the various test stress levels are shown. The total life includes the combined crack nucleation period and the fatigue-crack propagation period.

The rate of fatigue-crack propagation as affected by rate of cyclic loading and test-load frequency is an additional parameter to be considered. In elevated-temperature fatigue testing, it is known that the number of cycles to fracture decreases, and the crack-growth rate increases as the speed or frequency of cyclic loads is decreased (Figure B5). The damaging, thermally activated mechanism of creep or creep cracking, acting conjointly with fatigue, is responsible for this behavior. In general, this is true because, in the accumulation of stress cycles, slower rates of load cycling result in exposure of the metal to temperature for longer periods of time than in high-speed tests.

GROWTH OF FATIGUE CRACKS AS A
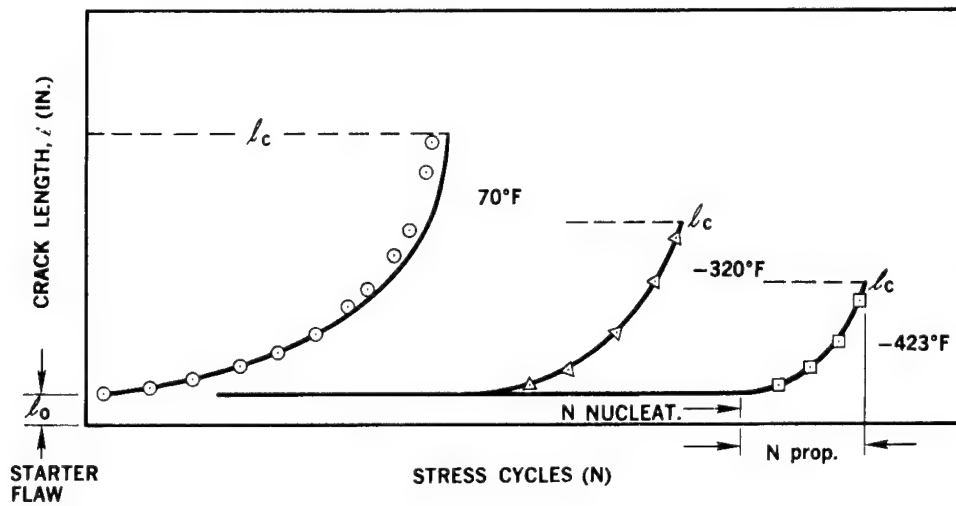# FUNCTION OF TEMPERATURE (SCHEMATIC)

Figure B1

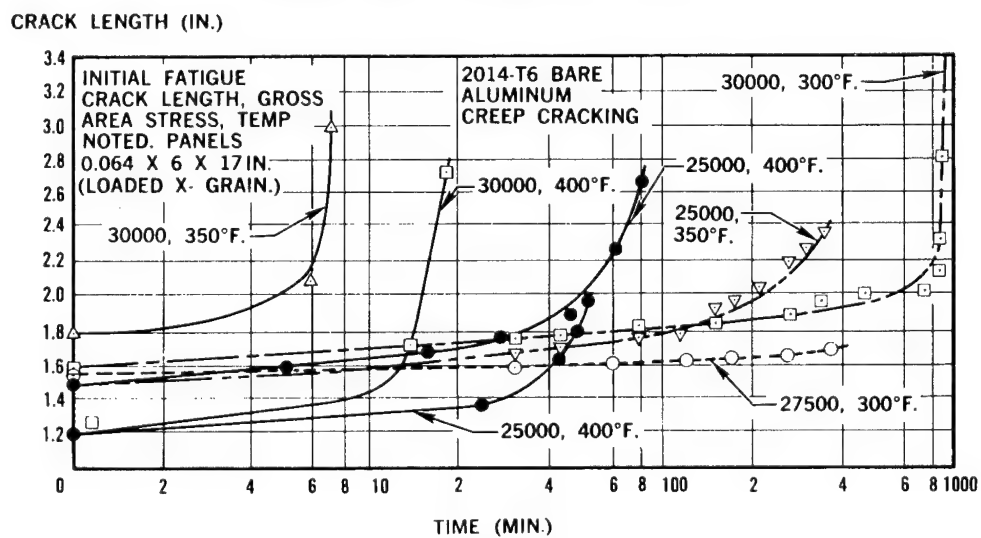# GROWTH OF CRACK UNDER STEADY
LOAD AND TEMPERATURE

Figure B2

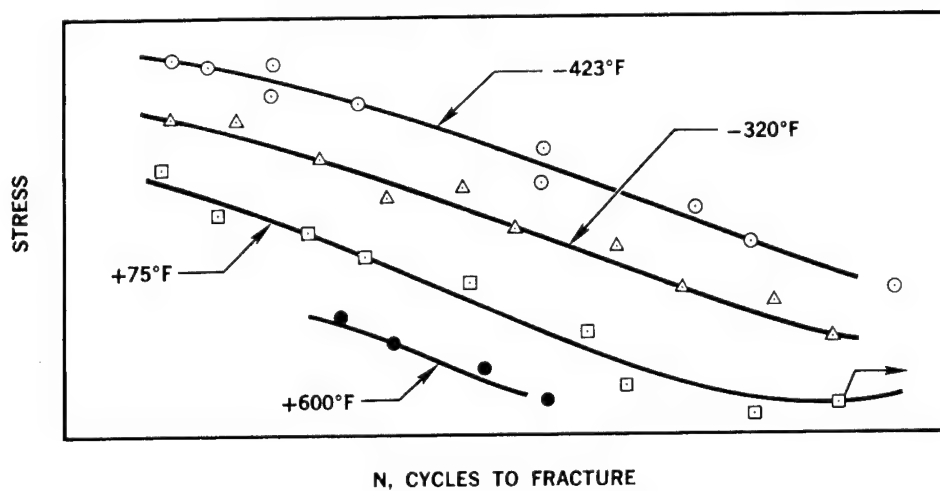# FATIGUE LIFE AS A FUNCTION OF TEST TEMPERATURE
(TYPICAL FOR MOST METALS)

N, CYCLES TO FRACTURE

Figure B3

EFFECT OF TEMPERATURE

AXIAL FATIGUE TEST
Ti-8Al-1Mo-1V, MILL ANNEALED
$K_T = 2.33$
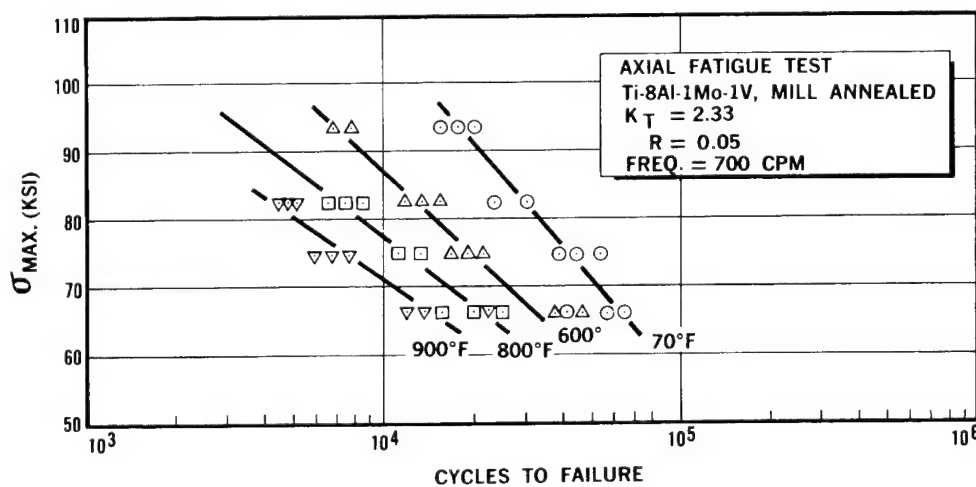$R = 0.05$
FREQ. = 700 CPM

CYCLES TO FAILURE

Figure B4

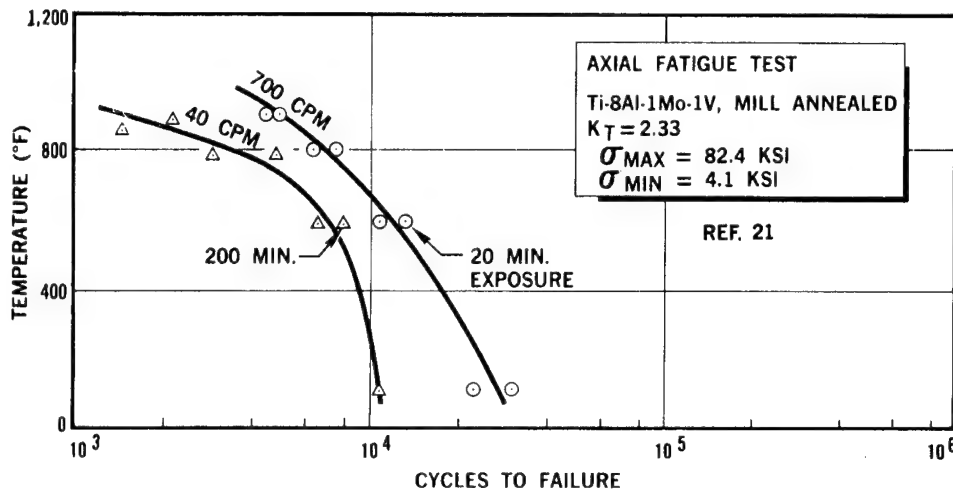## EFFECT OF FREQUENCY AT ELEVATED TEMPERATURE

IRD-950A

Figure B5

However, from cryogenic temperatures to room temperature, no damaging, thermally activated mechanisms are active. It is believed that fatigue lives and crack-growth rates at cryogenic temperatures will be independent of load frequency for most metals.

At elevated temperature both deformation and fracture under fatigue or static loading are time dependent, and the limitation on design stresses, imposed by deformation, becomes significant. A consistent set of data which can be used to show these effects is difficult to find. Reference 28 contains fatigue and deformation data for several alloys tested at high temperature. The deformation data do not encompass small deformations. However, the data presented for S-816 alloy are sufficiently comprehensive to permit extrapolation to determine approximately the stresses corresponding to 0.2% deformation. The data for fatigue failure and the extrapolated data for deformation were used to construct the curve presented in Figure B6. The figure is called a creep-boundary fatigue diagram. The solid curves are constant life lines
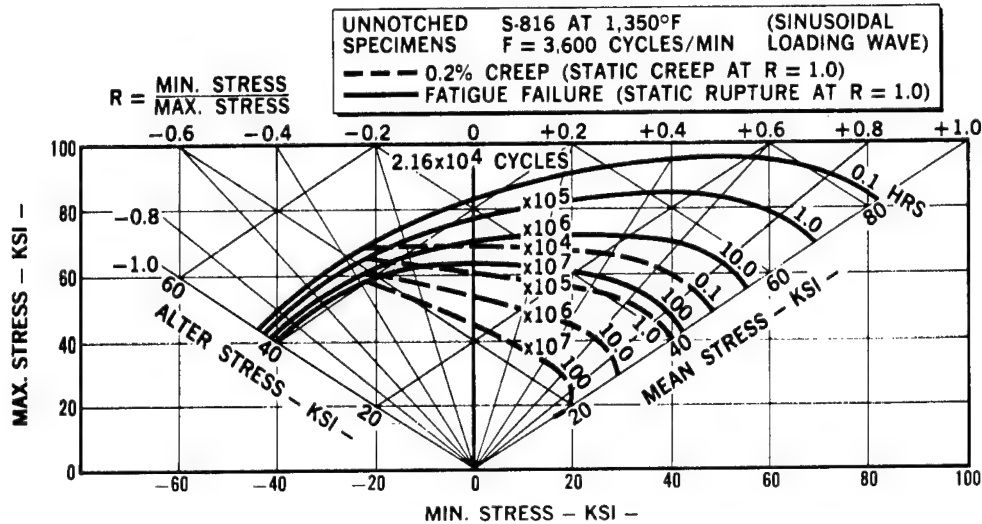
65

C-B FATIGUE DIAGRAM

for fatigue rupture and the dashed curves are constant life lines for 0.2% deformation. Figure B6 gives the fatigue failure and deformation data for S-816 alloy at 1350°F. The alloy is seen to be deformation critical at 1350°F at all R ratios higher than -0.3, and fatigue critical only at R ratios less than -0.3.

It is clear from Figure B6 that designers cannot be guided by fatigue failure data alone in making a judgment about the useful life of a structure when that structure is subject to loading at elevated temperature.

Fatigue failure data and data of deformation occurring under fatigue loading are both needed for the design of structure loaded at elevated temperature. New testing techniques are required to get these data. Deformation measurements will have to be made during the course of fatigue testing. This adds up to very expensive testing, and in the interest of keeping cost under control it is desirable to have some means of extrapolating test data.

It appears that master fatigue diagrams would be a useful means for the extrapolation of data over a wider range of temperature than would be used to obtain the data. If this technique is successful, it would make possible the gathering of data for a range of temperatures with a minimum of testing.

The Dorn parameter, Reference 29, has been a useful correlation means for relating time and temperature as a function of stress for some specific strain deformation or rupture. Thus, a master diagram would consist of a family of R curves for fatigue rupture and a second family of R curves for 0.2% deformation covering a temperature range established by the extrapolation permissible from the range of temperatures under which tests are made. Figure B7 is a master diagram for 0.2% deformation. This figure was obtained from the data presented in Figure B6.

Dorn's parameter takes the form

$$\theta = te^{-\frac{\Delta H}{RT}} \tag{1}$$

M-22512
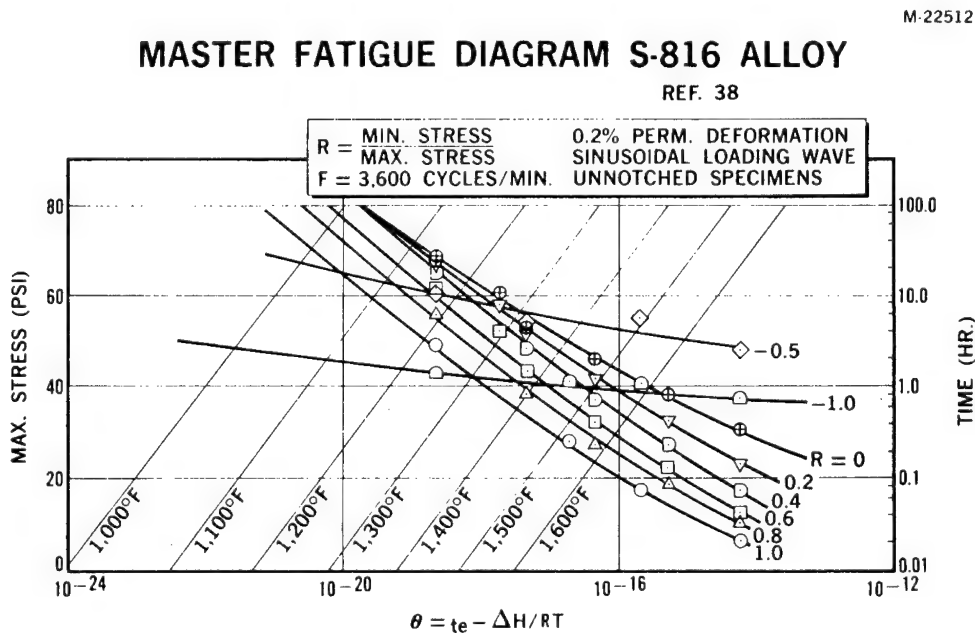

MASTER FATIGUE DIAGRAM S-816 ALLOY

REF. 38

Figure B7

67

where

ΔH = is the activation energy for creep or for rupture

R = is the gas constant

t = is the time

T = is the temperature in absolute units.

This master diagram permits one to relate the time to failure, for example, at one stress, temperature, and R ratio to another temperature at the same stress and R ratio.

Figure B8 shows typical test results of fatigue crack growth under mixed load ranges and cracking temperatures. These curves show significant changes in acceleration and deceleration of growth rate as the loading conditions are altered. Some success in predicting the behavior and crack length under a programmed set of conditions has been made. The techniques can be found in References 30 and 31. Techniques for predicting crack growth under random loading are discussed in Appendix D.

M-22517

FATIGUE—CRACK GROWTH UNDER PROGRAMMED LOADS
RATE OF GROWTH
(NOT LEVEL) =
LO-HI-LO-LO

STEP	σ MAX	R	$T_{CRK}°F$
1	20	0.5	235
2	20	0.2	70
3	*22.5	0.5	200
4	20	0.5	235

*NOTE INCREASE IN σ FROM STEP 2 TO 3, YET A DECREASE IN CRACK GROWTH RATE
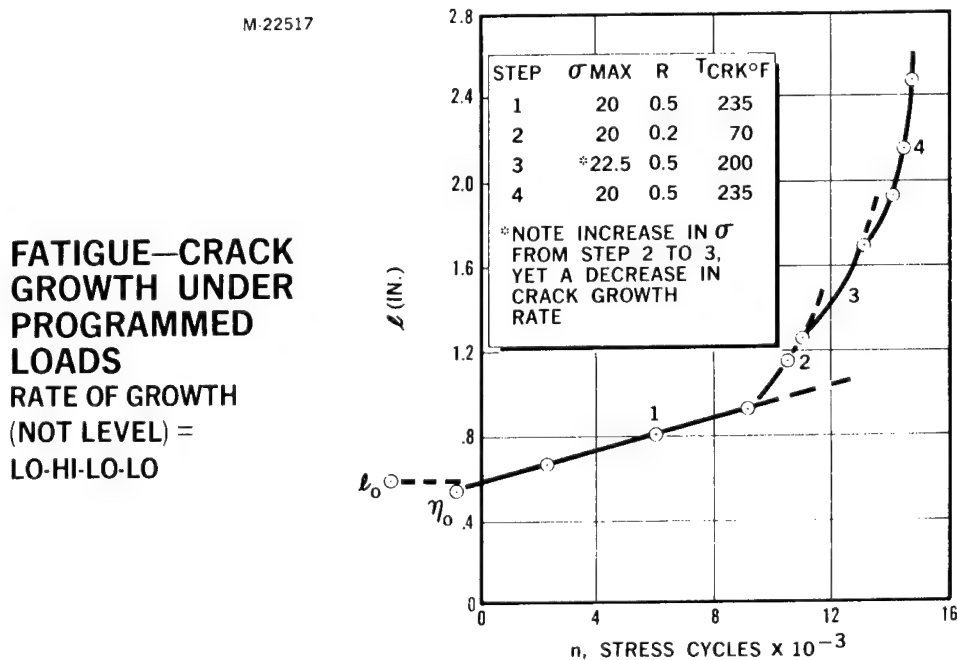
ℓ (IN.)

n, STRESS CYCLES x 10^{-3}

Figure B8

It is becoming increasingly clear that the crack-growth period in fatigue comprises a very large percentage of the total fatigue life. For this reason, more investigations are required to define the rate of crack progression, since these observations lead to a better insight concerning the progress in the accumulation of physical damage. Improvements to the non-linear damage concepts will result from this knowledge, and these modifications will result in more accurate predictions of structural behaviour.

The complex mechanisms of delayed cracking and delayed fracture, which occur under steady state rather than cyclic loading conditions, are additional subjects for investigation. The concept of a "critical strain level" for design operation should be pursued. Many of the high-strength steels for current and future use are particularly susceptible to the phenomenon of delayed fracture in the everyday corrosive environment of the atmosphere.

Figure B9 shows the results of testing one steel alloy in a mildly severe environment. It has been demonstrated that the form of the strength equation, shown on the graph, can be used for other environments.

In general, the fatigue life of a metal is longer in an inert atmosphere than in air. When its action is compared to that of inert gases, air is considered to be a corrosive environment. A decrease in corrosiveness of the environment results in less attack both on the surface of the metal and on the newly fractured surfaces generated in the process of fatigue cracking. Therefore, the greater the reactivity of the environment the more rapid the crack growth and the shorter the fatigue life. Figure B10 and B11 show the relative effects of various environments on an aluminum and titanium alloy.

In Figure B12 are the data from experiments testing the fatigue characteristics of low carbon steel mechanically strained within the influence of a strong magnetic field. Test loading of the metal coupons under cyclic conditions was applied in a uniaxial specimen direction and normal to the magnetic field axis. Poles of a 3000 gauss permanent magnet encircled the critical test section of the coupons and provided a high intensity magnetic induction. The fatigue life as well as the number of strain cycles required to generate a crack of a given

DELAYED FRACTURE (STATIC FATIGUE) OF AISI 4340 STEEL IN WATER ENVIRONMENT. (PH=.5 TO 1.0)

M-22516
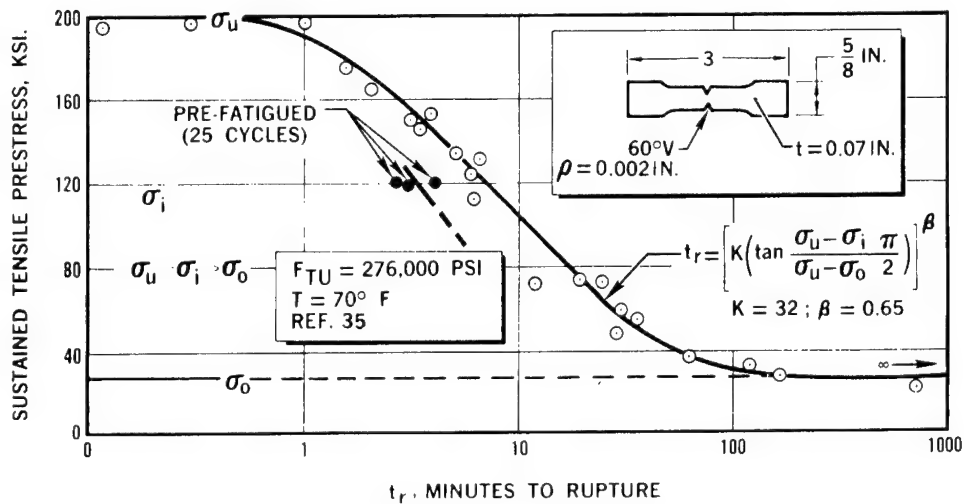

$$t_r = \left[K \left(\tan \frac{\sigma_u - \sigma_i}{\sigma_u - \sigma_o} \frac{\pi}{2} \right) \right]^{\beta}$$

$K = 32$; $\beta = 0.65$

$F_{TU} = 276,000$ PSI
$T = 70°$ F
REF. 35

t_r, MINUTES TO RUPTURE

Figure B9

CRACK GROWTH IN INERT GASES. GAS PRESSURES NOTED (MM. HG.)
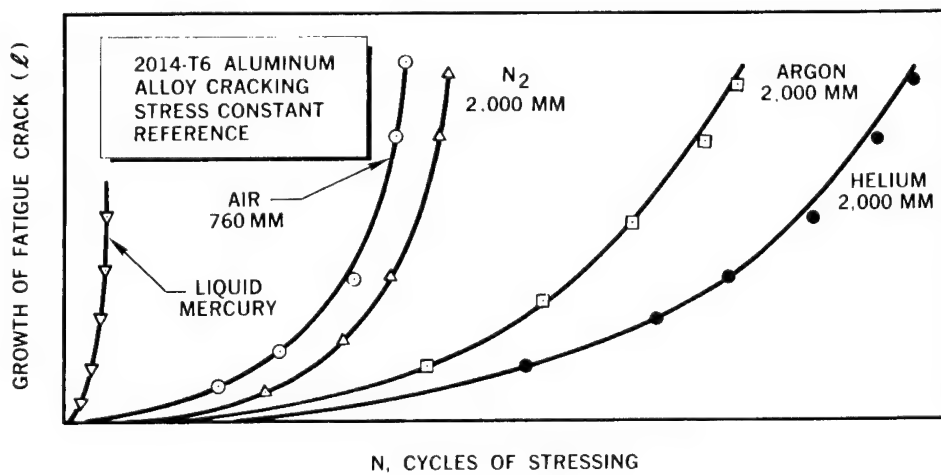
M-22513

N, CYCLES OF STRESSING
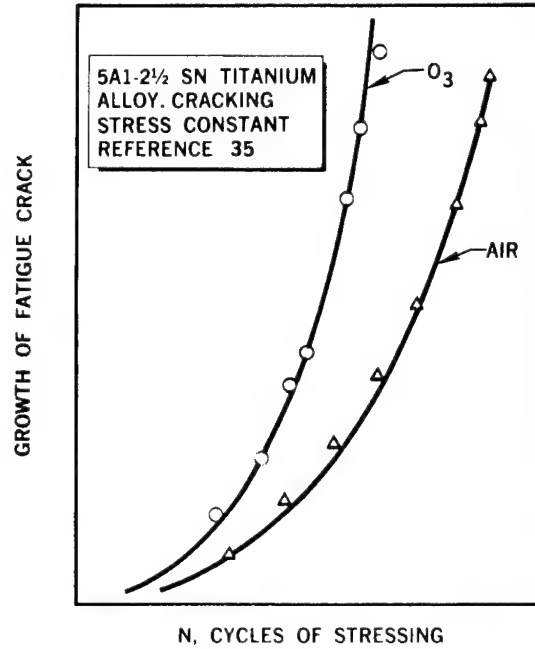
Figure B10

**CRACK GROWTH
OF TITANIUM
IN OZONE.**
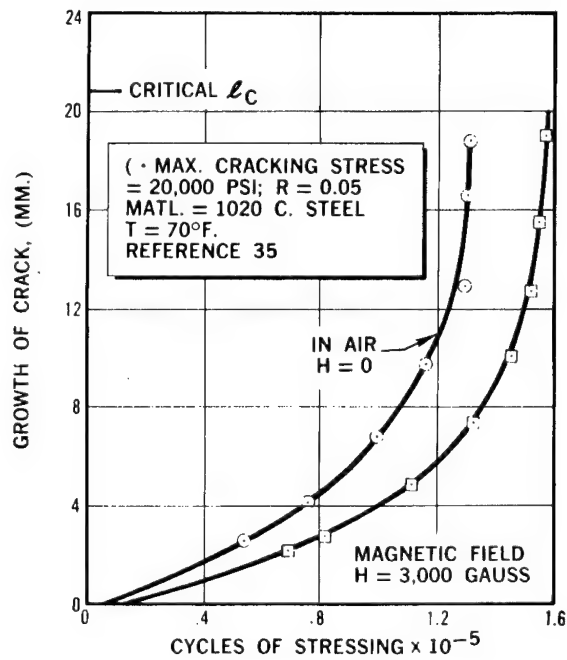

Figure B11

**FATIGUE OF
FERROMAGNETIC
MATERIAL.**

Figure B12

length was found to increase for the ferromagnetic material tested while within the field. Conversely, nonmagnetic aluminum alloy exhibited no differences in fatigue characteristics when tested either in or out of the influence of the magnetic field. In this example, neither magnetostriction nor magneto-elasticity are suggested as reasons for altering metal fatigue characteristics. Instead, magnetic induction of the strain cycled coupons was observed to magnetize and retain the metal debris generated during the fatigue cracking process. The debris became wedged between the mating crack surfaces and was shown by photoelastic techniques to mechanically reduce the stress intensity at the growing crack tip. The reduction in stress range by this mechanism was responsible for increases in fatigue life and reductions in crack growth rates.

Some investigations have been made on the effect of nuclear irradiation on mechanical fatigue properties of metals. Radiation-induced changes are usually referred to as radiation damage since in many cases the effects have been detrimental in one form or another. Damaging effects such as loss in ductility have been noted for many metals. Beneficial effects evidenced by increased yield and ultimate yields and ultimate strengths, fatigue strength, and surface hardening also have been noted. Rotating beam fatigue tests on 7075-T6 aluminum alloy shown in Figure B13 indicate an improvement in life due to the effects of a total integrated flux of 2×10^{18} fast neutrons/cm^2. Although the amount of irradiation received by the specimens in these tests is believed sufficient to alter mechanical properties, it is not known if the results are significant for the characteristics of metals during the conjoint action of fatigue straining and irradiation. Additional studies need to be undertaken for the simultaneous action of irradiation and mechanical straining at low temperatures.

It has been experimentally demonstrated (see Figure B14) that fatigue cracking under uniaxial direct stressing of an aluminum alloy occurs in hard vacuum almost as readily as within atmospheric pressure. This is contrary to general belief. Experiments now indicate trends toward increased crack growth rates which may eventually result in characteristics more critical than those from in-air tests. Results on aluminum continuously held in vacuum for periods

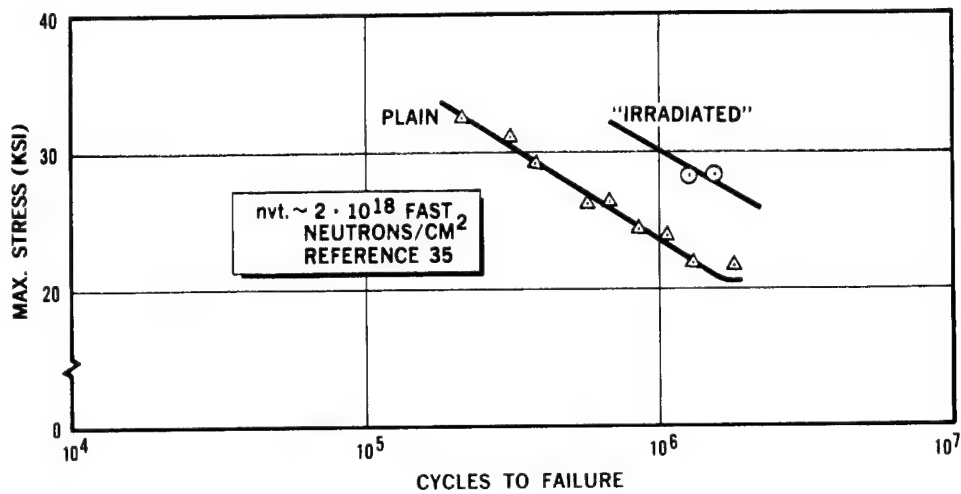## EFFECT OF PRIOR IRRADIATION ON UNNOTCHED 7075-T6 ALUMINUM ALLOY (ROTATING BEAM)
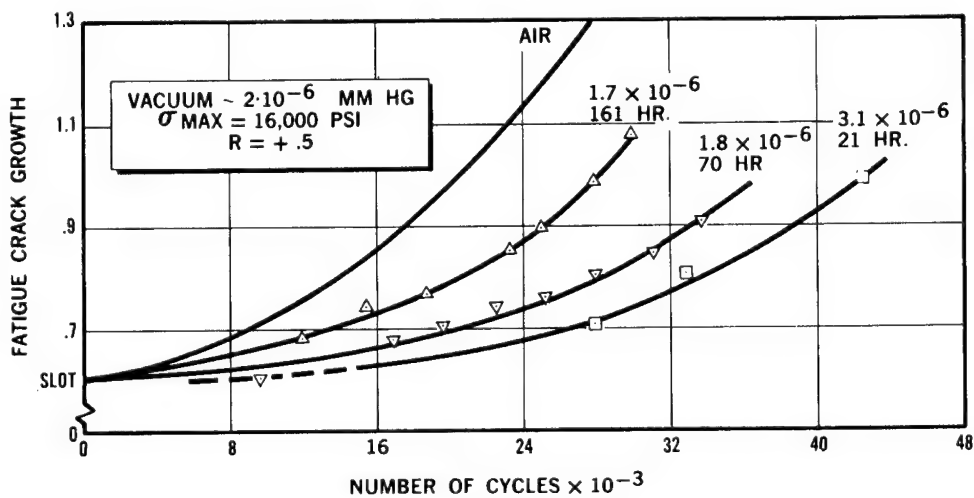

Figure B13

EFFECT OF OUTGASSING TIME

Figure B14

greater than a week yielded drastic reductions in fatigue properties. This strongly indicates the time dependency of the phenomenon. Results from short-time test exposures in vacuum as shown in Figure B15 showed improved properties. This is the usual accepted belief. However, for many cases an extension of the vacuum outgassing time is more a realistic environment than the short-time test exposures previously investigated. Because of this anomaly, prolonging the vacuum exposure is suggested as the only reliable procedure at present for evaluating metals for service in the space environment.

The possibility of a mechanism which can occur during partial out-gassing of the natural amorphous aluminum oxide film on the metal can be proposed to explain observed differences in the short-time as compared to long-time vacuum exposure tests.

The combined effect of vacuum and high temperature on fatigue life of a metal is shown in Figure B16. In the low-cycle-to-fracture range the fatigue life is
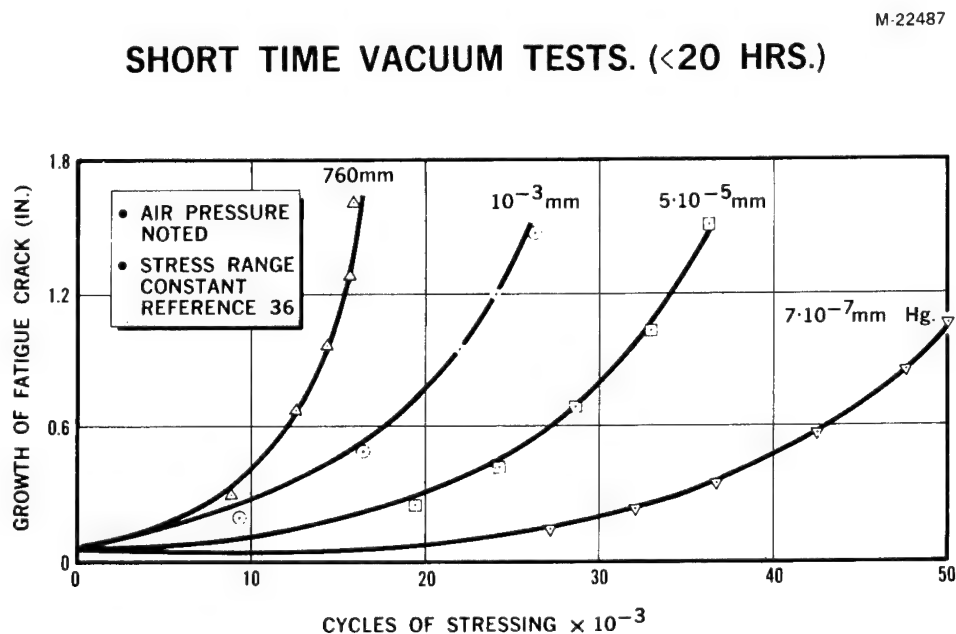
M-22487

SHORT TIME VACUUM TESTS. (<20 HRS.)

Figure B15

INFLUENCE OF ATMOSPHERE ON FATIGUE LIFE

REFERENCE 41

% PLASTIC STRAIN

NICKEL @ 816°C
R = −1.0
5 CPS

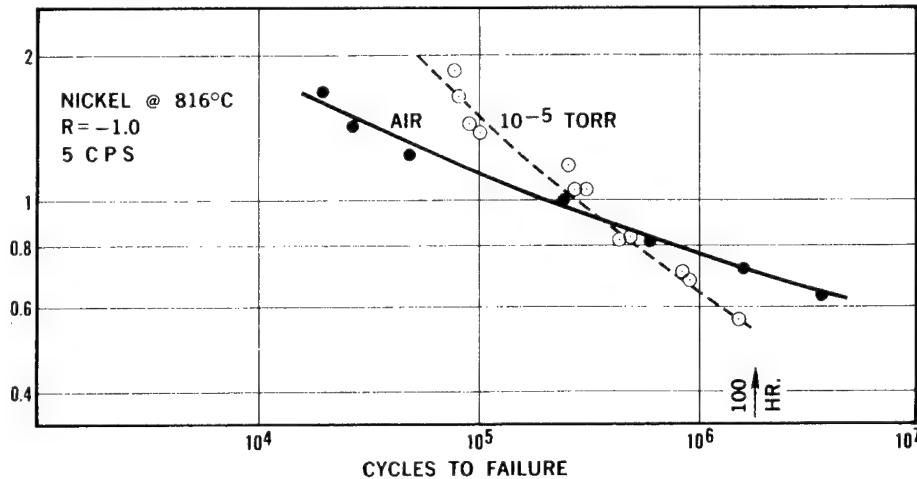AIR 10^{-5} TORR

100 HR.

CYCLES TO FAILURE

Figure B16

greater when tested in vacuum. As the stress level or cyclic strain range is reduced, a greater number of cycles are required to produce fracture. This increase in time to fracture results in longer exposure to vacuum, and in this region the fatigue life in vacuum is shorter than the life in air.

In summary, the preliminary results of many experiments have identified environments that enhance as well as degrade fatigue strength properties. One great difficulty in materials evaluation programs has been the inability to effectively simulate the environment. It is believed that the time-dependency of many material properties if not adequately explored will lead to invalid conclusions concerning the strength behavior of metals. In some cases, the results have been contradictory to generally accepted notions. These differences may be attributed to differences in the imposed conditions of laboratory tests.

Now, it is generally agreed that the effects of the space environments on engineering materials are largely unexplored and relatively unknown. Since useable mechanical properties of a metal in space are dependent upon "time" during the simultaneous action of the range in environments, we may have to rely on laboratory experiments conducted in space itself for the determination of some allowables.

APPENDIX C

FATIGUE LIFE, FATIGUE CRACKING AND RESIDUAL STRENGTH
OF FLAWED STRUCTURE UNDER BIAXIAL LOADING

The majority of structures which are designed, fabricated, and operated are subject to some degree of multiaxial or biaxial stressing while in service. Yet, major emphasis in evaluating the fatigue resistance of structure, by laboratory test, is placed on uniaxial loading methods. Evaluations by this method will in many cases result in unconservative designs and premature failure.

The fatigue of metals under multiaxial straining is a complex phenomenon. Factors which have contributed to this complexity are: loss in ductility, anisotropy, and texture hardening of materials. The effect of these factors on biaxial fatigue properties has not been adequately investigated. Therefore, at the current state of knowledge, it should be cautioned that the empirical characteristics defined for one material do not necessarily apply for others. For example, some materials have greater tensile strengths in the longitudinal rolling direction; others have higher strength in the transverse direction. Many of these same materials have higher biaxial strengths than uniaxial, yet when these materials contain flaws, the uniaxial strength can be greater than the biaxial strength. Also, to be considered is the value of the stress ratio of the biaxial principal strains. For some stress ratios the maximum principal strain may be normal to the weakest strength axis of the material. When the stress ratio is altered, it can be normal to the strongest strength axis of the material.

It is the purpose of this section to illustrate some fatigue characteristics of metals that are not well known or understood. In a few cases an awareness of these material properties existed but was neglected in design. The results were catastrophic. Figures C1 and C2 shows biaxial S-N curves for two aluminum alloys. In both examples, the biaxial straining conditions resulted in lower fatigue allowables than unidirectional straining.

Figure C3 illustrates the trends in fatigue crack growth as a function of loading. The test results were obtained on the aluminum alloy 2014-T6 for

BIAXIAL SN CURVES FOR 24ST EXTRUDED TUBES, (NACA 1889)
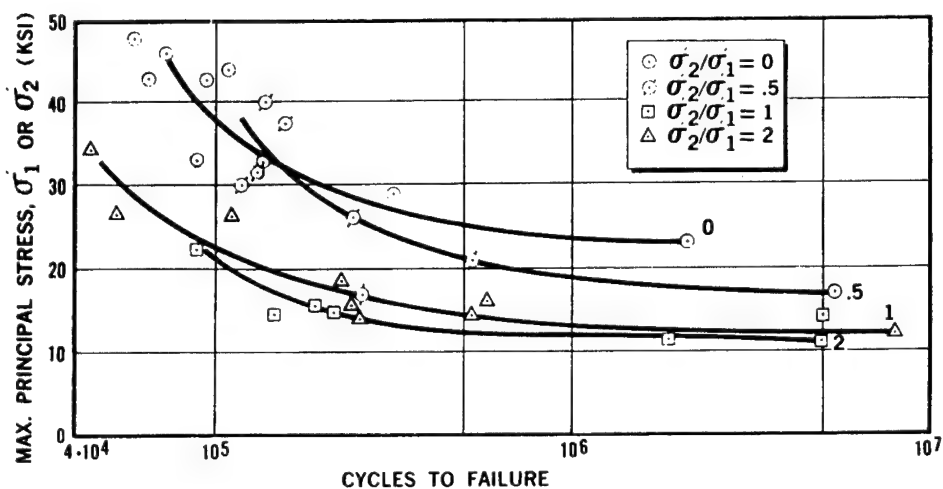
M-22491

Figure C1

M-22490

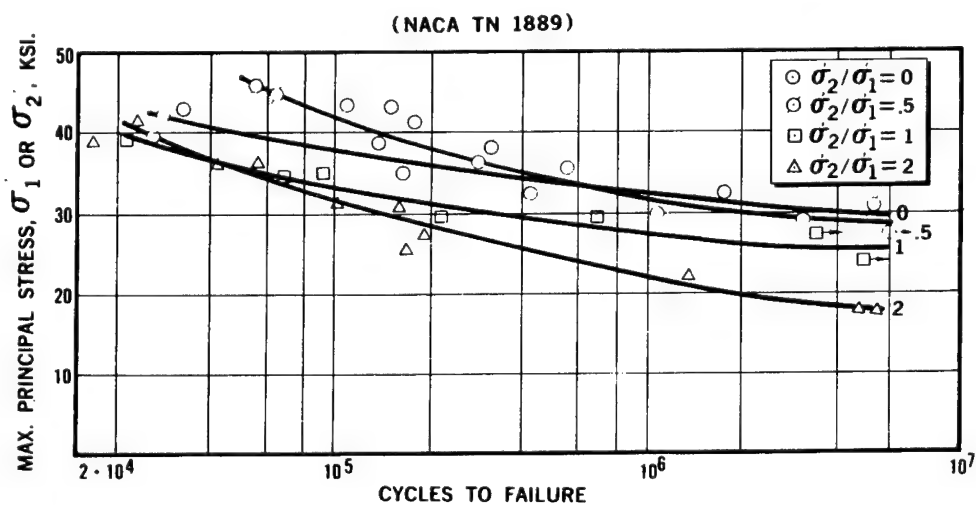## BIAXIAL SN CURVES FOR 14ST-4 TUBING

(NACA TN 1889)

Figure C2

78

two conditions of biaxiality as well as under uniaxial loading. The increased crack growth rates and shorter fatigue lives under biaxial loading agree with the trend in fatigue lives in Figure C1.

Unless otherwise noted, the nominal maximum principal stress for all specimen configurations on Figure C3 was 14,000 psi. The biaxially loaded plate (2:1 stress field) appears to have a slower crack growth rate than the pressurized cylinder (2:1 stress-field). This is reasonable, since the membrane stress field in the simple-supported plate is variable and diminishes as the crack extends and approaches the edge of the plate specimen. The nominal stress field in the pressurized cylinder and uniaxially loaded plate on the other hand is constant.

Figure C3 also shows the differences in crack growth rate as a function of anisotropy. It can be seen from the figure that the slowest rate of crack growth occurs when the crack is propagating normal to the material rolling direction. The reader again is cautioned that this rule is not meant to be applicable for all materials. There are unpublished data indicating an opposite rule for some titanium alloys.

Figure C4 shows the fracture strength as a function of anisotropy on flawed 2014-T6 plates. Fatigue cracks 1.8-in. long were grown in the 6-in. wide uniaxial loaded plates of Figure C3. These plates were then ruptured at 75° and -320°F. If the fracture strengths in the longitudinal and transverse direction are known, it is possible to calculate the strength for other orientation angles of flaw-to-grain direction by the simple expression

$$\sigma_{\theta = i°} = \sigma_{0°} - \sin\theta\,(\sigma_{0°} - \sigma_{90°}) \tag{1}$$

Small undetected and/or accidental flaws can promote catastrophic rupture in pressure vessels at stresses far below design levels. Designers and inspectors require knowledge concerning the size of small flaws, and their gradual extension by fatigue action, that may lead to instability from loads incurred by proof testing or in service. This information is necessary in order to define safe limits for the working stresses in structure. One method
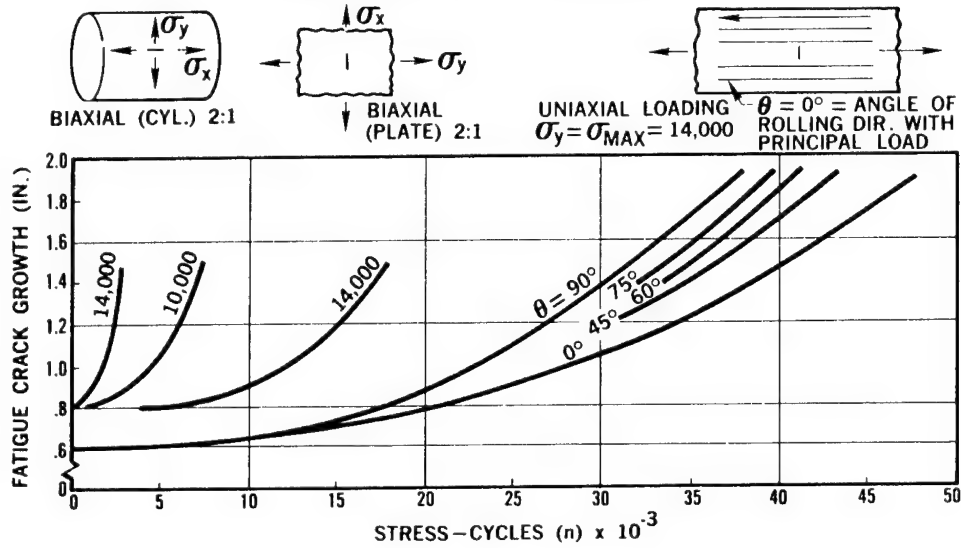
FLAW GROWTH UNDER UNIAXIAL AND BIAXIAL LOADING

Figure C3

FRACTURE STRENGTH AS A FUNCTION OF FLAW ORIENTATION

θ = ANGLE LOAD DIRECTION TO ROLLING DIRECTION

ϕ = ANGLE FATIGUE CRACK TO ROLLING DIRECTION

$\phi = 90° - \theta$

$90°$ = ANGLE CRACK TO LOAD. (CONST.)

$$\sigma_{\theta = i} = \sigma_0 - \sin\theta \left(\sigma_0 - \sigma_{90} \right)$$
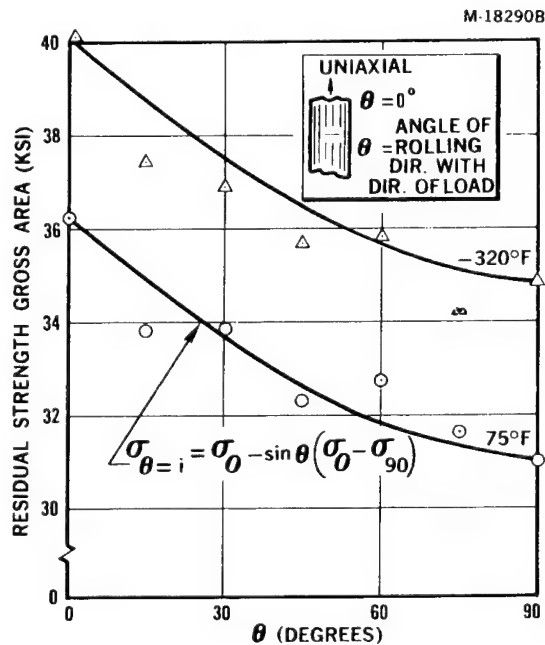
Figure C4

of obtaining this information in the laboratory is by rupturing structural
panels in various widths and sizes and containing fatigue cracks.

Figure C5 shows the fracture strength or residual strength of some uniaxially
loaded panels of aluminum alloy 2014-T6 in a variety of widths and crack
sizes. Data for any one panel size can be represented by the equation

$$\sigma_R = \frac{\sigma_u \left(1 - \frac{\ell c}{w}\right)}{\sqrt{1 + \frac{3\ell c}{R'_p}}} \qquad (2)$$

where

$$\sigma_R = \text{residual strength (cracked)}$$

$$\sigma_u = \text{ult. tensile strength (uncracked)}$$

M-18286A

PREDICTION OF FRACTURE STRENGTH OF
FLAWED STRUCTURE UNDER BIAXIAL LOADING
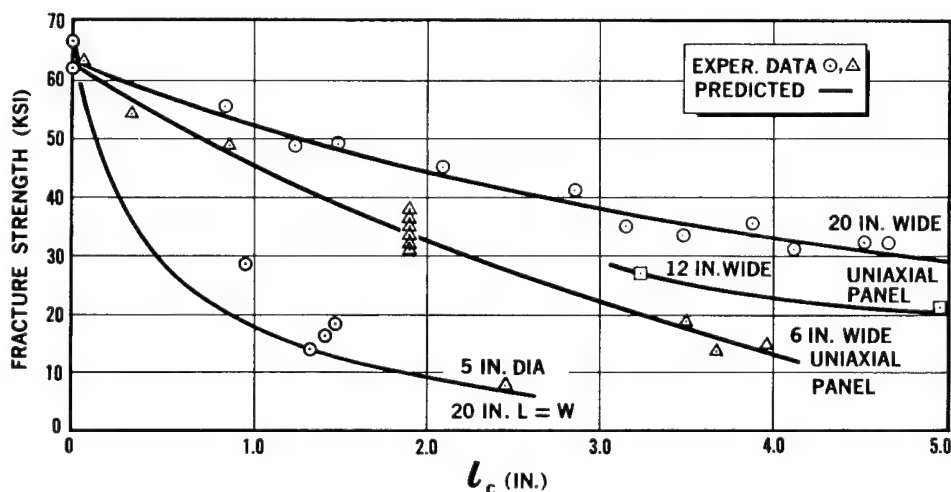
Figure C5

$$\ell_c = \text{length of crack}$$

$$W = \text{panel width}$$

$$R_p{}' = \text{empirical constant determined from test (figure C-7)}$$

The fracture envelopes for other widths of panels can be calculated from this equation by substituting appropriate values of W into the formula. The value of $R_p{}'$ remains constant for a given material in a given temper and fabricated condition. The derivation of this equation is given in Reference 30. Good agreement between calculated and experimental results are shown in Figure C5.

The equation can also be modified to predict the behavior of flawed structure under biaxial loading. It is first necessary to calculate the fracture envelope of uniaxially loaded panels in a width equal to the length of the cylinder in question. The fracture strength of the cylinder is then calculated from:

$$\sigma_{\text{hoop}} = \frac{\dfrac{\sigma_u \left(1 - \dfrac{\ell_c}{w}\right)}{\sqrt{1 + 3\,\dfrac{\ell_c}{R_p{}'}}}}{\left[1 + 4.6\,\dfrac{\ell_c}{\text{radius}}\right]^{*}} \qquad (3)$$

*Kuhn (Reference 32)

The lower curve in Figure C5 has been calculated from this equation and shows good agreement with test data on 5 in. -diameter cylinders 20 in. long.

Another example of the usefulness of this equation in design is shown in Figure C6. In this example, cracked test panels 12 in. in width and of the same structural configuration were ruptured in uniaxial tension. From these data,
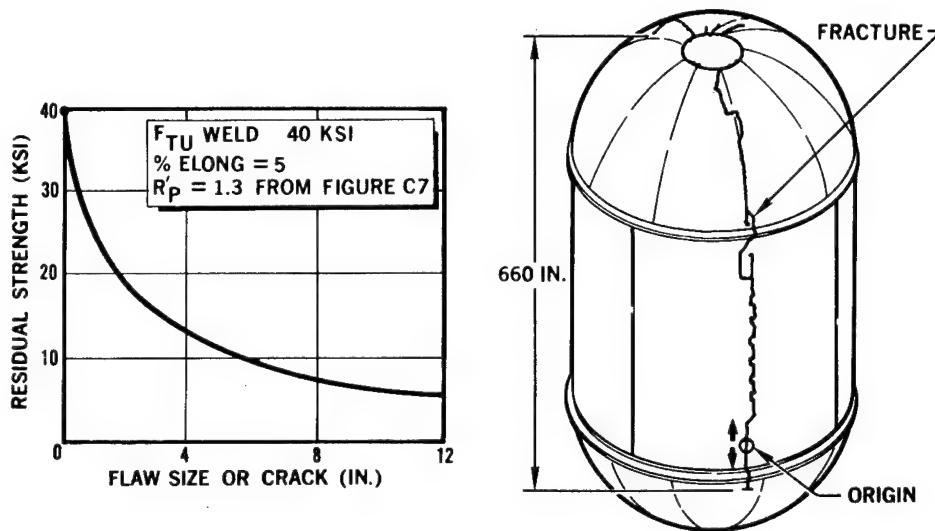
S-IV B HYDROSTATIC BURST
TEST SPECIMEN

M-18288A

Figure C6

the fracture envelope for a 660-in.-long cylinder was calculated and then modified for biaxial loads and radius of curvature effects with Kuhn's correction factor (Reference 32).

Nominal values of σ_u and R_p used in the equation were obtained from coupon tests of weld metal properties because fracture initiated at a flaw in the weld seam. The hoop stress at burst for the 130-in.-radius vessel was 13,000 psi. The predicted fracture envelope in Figure C6 at this stress defines a critical flaw size of 4 in. Post-test examination of the fractured tank revealed a flaw (termed incomplete fusion) in the weld seam over 3-1/4 in. in length.

Such close agreement between actual and predicted behavior suggests that the analysis method can be used in design. Additional data that would be useful to the designer would be the rate of growth of such flaws with pressure cycles. The decrease in strength of pressure vessels from cycling in operation could then be expressed as shown in Figure G-1 of Appendix G.

83

NOTCH RESISTANCE AS A FUNCTION OF MATERIAL DUCTILITY (FOR FATIGUE CRACKED STRUCTURE)

M-22496

% ELONGATION IN 2 IN. GAUGE LENGTH (BY TEST)

R'_p, PLASTIC ZONE NOTCH RESISTANCE FACTOR

ALUMINUM ALLOYS
TITANIUM ALLOYS
STEEL ALLOYS
SEMI-AUST. STEEL ALLOYS
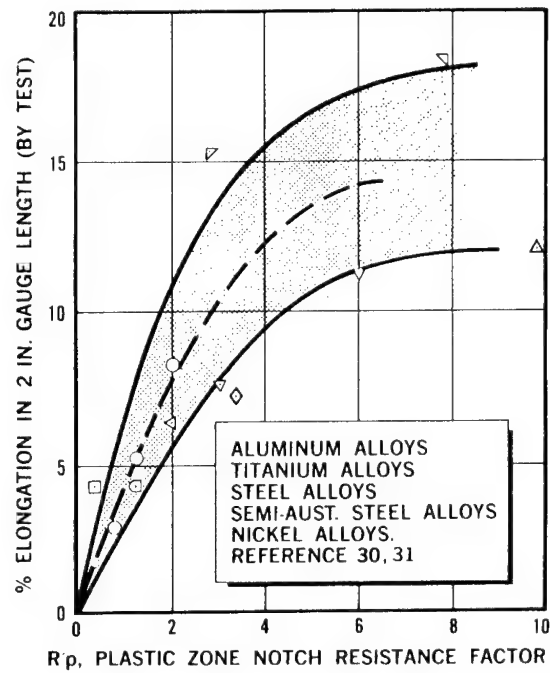NICKEL ALLOYS.
REFERENCE 30, 31

Figure C7

APPENDIX D

FATIGUE CHARACTERISTICS
UNDER RANDOM LOADING

In this section, working examples are given of acceptable methods for predicting fatigue characteristics of structure subjected to random loads from laboratory test results under sinusoidal constant amplitude loading. In the first example, fatigue lives of samples under random loading are calculated from known fatigue lives under discrete loading. The calculated lives are then compared to experimentally determined lives under random loading. Good agreement between predicted and experimental results show the method to be satisfactory for use in design.

In the second example, a similar method is outlined for the prediction of fatigue crack growth under random loads. By this technique it is believed that additional accuracy in predicting fatigue life will result. The best indication at present for the rate of nonlinear damage accumulation in structure is from the observed crack-growth characteristics. Future experiments should be designed to gather this information. Now, if the total damage to fracture is integrated over small increments of time to grow a crack to a given length, and these increments during crack extension are successively added along the observed nonlinear path of physical damage accumulation, then the calculated time to failure will be precise.

Fatigue Life

Figure D1 shows the fatigue test results for notched aluminum specimens under both sinusoidal constant amplitude loading and random noise. The data has been taken from Reference 26.

Table D1 shows the analysis technique for calculating the proportion of peak stresses experienced in a random process. The Rayleigh probability distribution function is used and will accurately predict the number of occurrences for simple one-degree-of freedom systems within relatively narrow bands of load frequency.

SINUSOIDAL AND RANDOM SN DATA

ALTERNATING STRESS (KSI)

DATA FROM REFERENCE 26

SINE WAVE TESTS. MEAN SN CURVE

MIN. SN CURVE

σ_{RMS} = 11,260 PSI →

△ SINUSOIDAL CONST. AMPLITUDE (N VS. ALTERNATING σ)
○ RANDOM NOISE (N VS. RMS STRESS)

N, CYCLES TO FAILURE
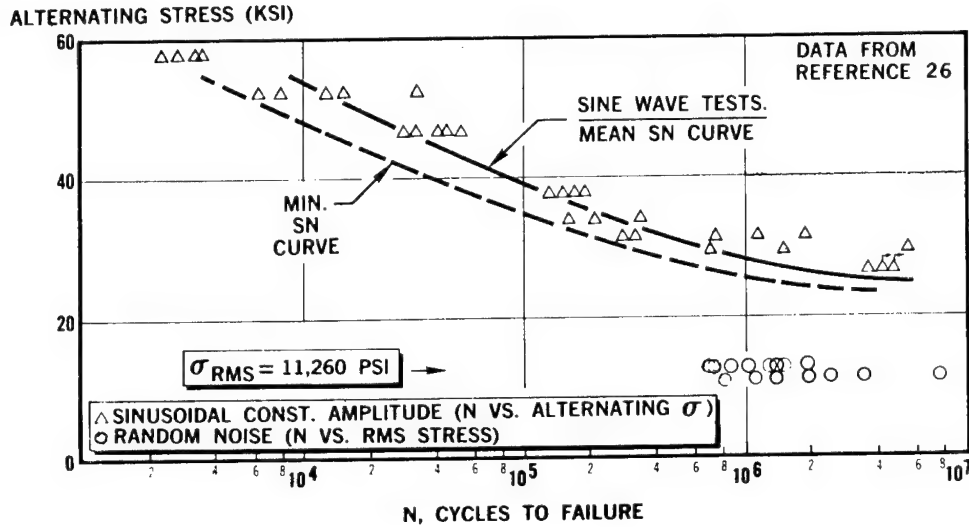
Figure D1

In this exercise, a class interval of one-third has been used for the value of ΔX.

Use Rayleigh probability distribution function for prediction of peak stress proportionment in random process

$$P_{(x)} = xe^{-\frac{x^2}{2}} \tag{1}$$

where

$$x = \text{ratio of } \sigma \text{ peak to } \sigma_{R.M.S.}$$

Then, number of cycles under random loading, N_R, can be calculated from,

$$\frac{1}{\bar{N}_R} = \int \frac{P_{(x)} dx}{N_{(s)}} \simeq \sum \frac{xe^{-\frac{x^2}{2}} \Delta x}{N(s)} = \frac{1}{\text{random load cycles to failure}} \tag{2}$$

86

where

$N_{(s)}$ = cycles to failure under sinusoidal const., amplitude at discrete values of (x)

Δx = 0.33 weighting factor (choose $\Delta x = 1/3$ class interval)

Table D1 shows results of the numerical calculations which are required to predict the number of cycles to failure (N_R) for random load excitation. Two sets of calculations are made, one based on the minimum S-N curve and the other on the average S-N curve in Figure D1.

Table D2 shows the comparison between predicted and actual experimental results.

Fatigue Crack Growth

Structural test articles may be tested to several discrete stress levels under constant amplitude loading. Each sample is to be subjected to only one range of cyclic stressing. Nine discrete stress ranges may be chosen for these tests, corresponding to nine values of (x), where (x) equals the ratio of peak stress to root-mean-square stress within a cycle. Test stress levels of (x) from 0.67 to 3.33 may be selected. During these tests, the growth of the fatigue crack should be recorded as a function of the number of stress cycles. Typical data are illustrated in Figure D2. Experimental results of this kind depict the nonlinear nature of damage accumulation more accurately than the results obtained by the measurement of total number of cycles to fracture.

From these data, fatigue-crack growth under random loading then may be calculated in a manner similar to that used for fatigue life. The number of cycles of random loading, n_{r_i}, required to generate a crack equivalent in length to the same length of crack produced under discrete loadings is calculated from:

Table D1. CALCULATIONS FOR RANDOM FATIGUE LIFE

X	σ peak (psi)	Average From Fig. D1 $N_s \times 10^{-6}$	$Xe^{-X^2/2}\,\Delta X$	$\dfrac{Xe^{-X^2/2}}{N_s}\Delta X \cdot 10^{-6}$	Minimum From Fig. D1 $N_s\,10^{-6}$	Xe $Xe^{-X^2/2}\,\Delta X$	$\dfrac{Xe^{-X^2/2}}{N_s}\Delta X \cdot 10^{-6}$
1	11260	∞	.202	0	∞	.202	0
1-1/3	15010	∞	.182	0	∞	.182	0
1-2/3	18760	∞	.140	0	∞	.140	0
2	22520	∞	.091	0	100	.091	.00091
2-1/3	26270	1.08	.0518	.04800	.75	.0518	.06910
2-2/3	30020	.62	.0255	.04120	.27	.0255	.09450
3	33780	.30	.0111	.03700	.14	.0111	.07920
3-1/3	37530	.15	.0044	.02940	.066	.0044	.06670
3-2/3	41280	.075	.00149	.01990	.032	.00149	.04650
4.0	45040	.040	.000402	.00100	.017	.000402	.02360
			$\sum =$	.17650		$\sum =$	.38051

Predicted $N_R = \dfrac{1}{.1765 \times 10^{-6}}$ = 5,660.000 cycles
Based on avg. sine SN curve.

Predicted $N_R = \dfrac{1}{.3805 \cdot 10^{-6}}$ = 2,630,000 cyc.
Based on minimum sine S-N curve.

σ_{RMS}	Experimental Fatigue Life under Random Noise (cycles) Reference 26	Predicted Fatigue Life (cycles) Table D1
11,260 psi	2,020,000	2,630,000
	1,380,000	
	2,490,000	
	850,000	
	1,110,000	
	7,890,000	5,660,000
	3,410,000	

2,730,000 = avg. 7

Ratio $\dfrac{\text{predicted}}{\text{experimental}}$ = 0.96 to 2.07

FATIGUE CRACK GROWTH UNDER DISCRETE AND RANDOM CYCLIC LOADING

Figure D2

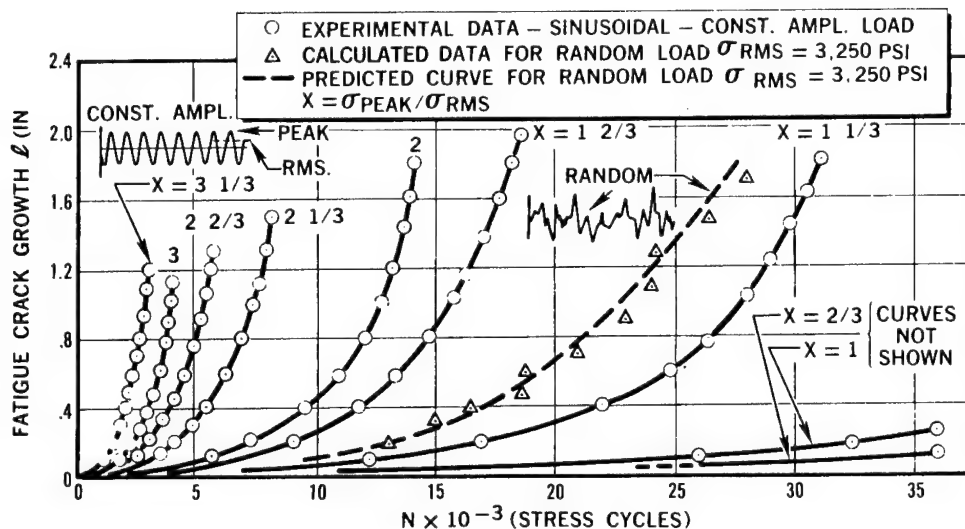$$
\frac{1}{nr} = \int_{\ell=o}^{\ell=i} \frac{xe^{-\frac{x^2}{2}} \, dx}{n_{(x)}} \simeq \sum_{\ell=o}^{\ell=i} \frac{x_i \, e^{-\frac{x^2}{2}} \, \Delta x}{n_{(xi)}} = \frac{1}{nr_i} \quad (3)
$$

where

$$x = \frac{\text{peak stress}}{\text{rms stress}}$$

Δx = 0.33 class interval in Rayleigh distribution function defining peak stresses in discrete amplitude loading tests

$n_{(x_i)}$ = number of cycles to successively grow crack from $\ell = 0$ to $\ell = \ell_i$ to $\ell = \ell_j$ etc., under constant amplitude, sinusoidal loading.

To check the validity of the above analysis, the next objective should be to conduct a random cyclic load test. During the test, measurements are to be taken of the growth of the crack wherever it may occur in the sample. Hypothetical results are shown in Figure D2. It should be noted that this technique may reveal the nonexistence of a single stress-producing damage at a rate equivalent to that measured under random loading. This contradicts previously accepted beliefs. It is realized that the assumption that an equivalent damaging stress level did exist has been made in the past because of the lack of experimental proof.

Additional experiments are necessary. Encouraging results from such programs will indicate that a series of less costly discrete tests can be used to predict behavior of structures subjected to random loads.

FRACTURE-SAFE DESIGN OF SPACECRAFT STRUCTURES
(SPACE CABIN RELIABILITY)

Statement of Problem

Inadvertent damage to spacecraft structure can occur during the operation of a vehicle. The damage can come from a variety of causes such as: (1) meteoroid penetration (point of impact or dispersed through shield), (2) undetected flaws and cracks during fabrication, (3) components flung from runaway (internal) machinery, (4) minor collisions, (5) fatigue cracks generated from high-frequency loading and high stresses during the launch phase of flight, (6) material degradation in the space environment (long-time), (7) acts of demented passengers and accidental damage, (8) damage from the effects of blast loads.

Initial damage incurred through any of these causes can promote explosive decompression and complete loss of a highly stressed and pressurized vehicle. However, the extent of damage or fracture can be partially controlled by the proper choice of working stresses in combination with sufficient structural reinforcement. The importance of vehicle reusability, and retrieval of personnel, equipment, and data necessitates the solution to this problem through improved design.

Current Experience

The current analysis and testing procedures used to define the fracture strength of flawed structure are adequate for design purposes. The methods now take into account the effect of biaxial loads on structure. In the past, the strength of structure often was determined directly from the results of uniaxial load tests which were adequate. Now, it has been demonstrated that biaxial or multiaxial loads are far more severe for the case of cracked structure. The successful designs produced, however, were in aircraft structure. The application of the present design methods to all welded spacecraft pressure vessels will require some additional investigation, although a carryover of past knowledge and experience will be helpful.

Approach

An acceptable approach for the evaluation of safe-structure by analysis and test which has been used in the past is as follows:

1. Determine the fracture envelope of the materials of construction. This can be presented as a variation in the strength of the material possessing various flaw sizes. The envelope can be obtained from uniaxial or multiaxial load tests, whichever is appropriate.

2. If the structure to be evaluated is extremely large, and necessitates a costly test program, then smaller test articles may be used. Semi-empirical equations are available for calculating the behavior of large structure from the results of small coupons. Formulas are also available for predicting the behavior under biaxial loads from the results of uniaxial load tests. Figures C5 and C6 of Appendix C demonstrate the success of the analytical methods and show close agreement between experimental and analytical results. Figure C5 shows good agreement between predicted and actual fracture strengths of flawed and small pressure vessels from the results of simple uniaxially loaded panels. Figure C6 shows the fracture envelope for a 260-in.-diameter pressure vessel which has been predicted from the results of 12-in. wide uniaxially ruptured panels.

3. The next step in evaluating a fracture-safe design is the determination of the structural reinforcements and the associated reductions in stress levels at the reinforcement that will arrest the fail-safe fracture. Figure E1 shows some actual experience in various structures. The existence of three regions should be noted. In the first region, the stresses are unnecessarily low and the cracks and flaws are nonpropagating. This region results in an overweight design. The middle region is acceptable, and within this boundary, cracks may develop into rapid fracture but the fracture is controlled and arrested. The control of the fracture is a function of the working stress and the structural reinforcement. The upper region is not acceptable for design, since fracture arrest is impossible. An alternate means of depicting the data of Figure E1 is shown in Figure E2. In this graph, the variation in residual strength with flaw size is shown as a function of structural reinforcement. It should be noted that higher allowable working stresses can be used with greater amounts of reinforcement.

4. A final analysis for the proper choice of ductile materials and attachments is required. In addition, a tradeoff study should be made by comparing the weights of structurally reinforced panels as a function of their design working stresses. The results of such a study can be depicted as shown in Figure E3. In the figure, the optimum design weight is plotted as a function of structural reinforcement.

M-22529
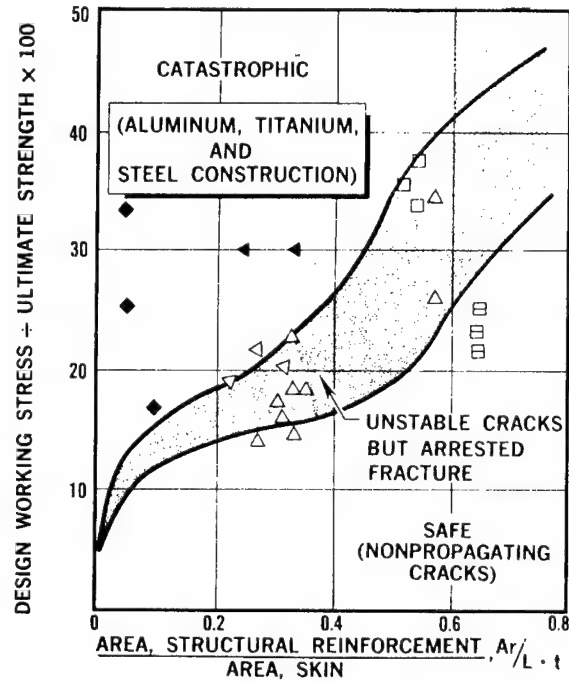
BOUNDARY
BETWEEN
CATASTROPHIC
AND
FRACTURE-SAFE
DESIGN

DESIGN WORKING STRESS ÷ ULTIMATE STRENGTH × 100

CATASTROPHIC

(ALUMINUM, TITANIUM,
AND
STEEL CONSTRUCTION)

UNSTABLE CRACKS
BUT ARRESTED
FRACTURE

SAFE
(NONPROPAGATING
CRACKS)

$$\frac{AREA,\ STRUCTURAL\ REINFORCEMENT}{AREA,\ SKIN},\ \frac{A_r}{L \cdot t}$$

Figure E1

SAFE-FRACTURE AS A FUNCTION OF
REINFORCEMENT AREA

M-22500

RESIDUAL STRENGTH (KSI)

UNSTABLE
CRACKS
(LOSS OF STRUCTURE)

$A_r/Lt = 0.54$

SAFE
FRACTURE

STABLE
CRACKS
(NON-PROPAGATING
UNDER STEADY-STATE LOADS)

$A_r/Lt = 0.32$

(CRACKS ARRESTED
AFTER ONSET)

• ALUMINUM ALLOY CONSTRUCT'N.
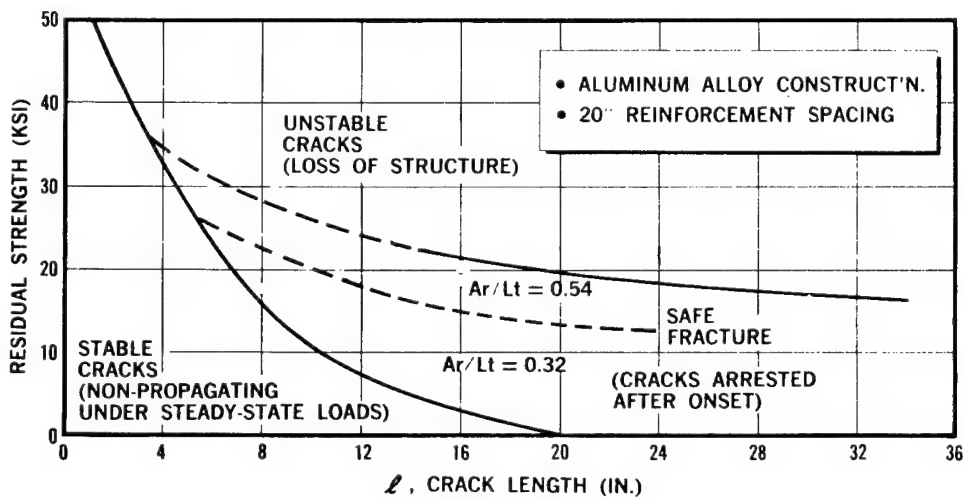• 20″ REINFORCEMENT SPACING

ℓ, CRACK LENGTH (IN.)

Figure E2

95

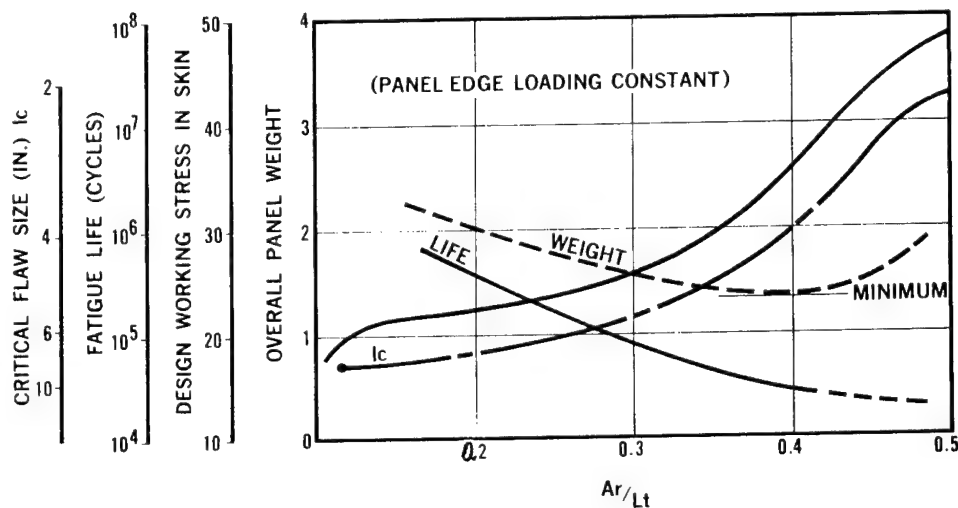## OPTIMUM WEIGHT VS. STRUCTURAL REINFORCEMENT
FOR FRACTURE-SAFE DESIGN

Figure E3

It would appear, however, that the optimum fracture-safe design for space-craft structure would be highly stressed skins and closely spaced structural reinforcements. Fatigue life is an additional parameter to be checked. In Figure E3, it should be noted that the optimum design weight structure for a fracture-safe design does not possess the optimum life. If increased fatigue life is an important consideration for a given design, then a heavier structure will be required. The concept of an allowable flaw size, even though arrested, may be another design consideration. For this case, an alternate off-optimum design weight will have to be chosen.

Recommendations for Future Research

It has been mentioned previously that the design of safe-structure has been most successful in the aircraft field. The structural reinforcements that have provided the mechanism for fracture arrest are shown as Item A and B in Figure E4. No experience is available for the few samples shown as Item C-F (Figure E4). However, it is believed that each of these configurations will provide some degree of fracture arrest. The amount of cross-sectional area of reinforcement and its associated reduction in stress level at the reinforcement in order to arrest fracture, will have to be empirically determined.
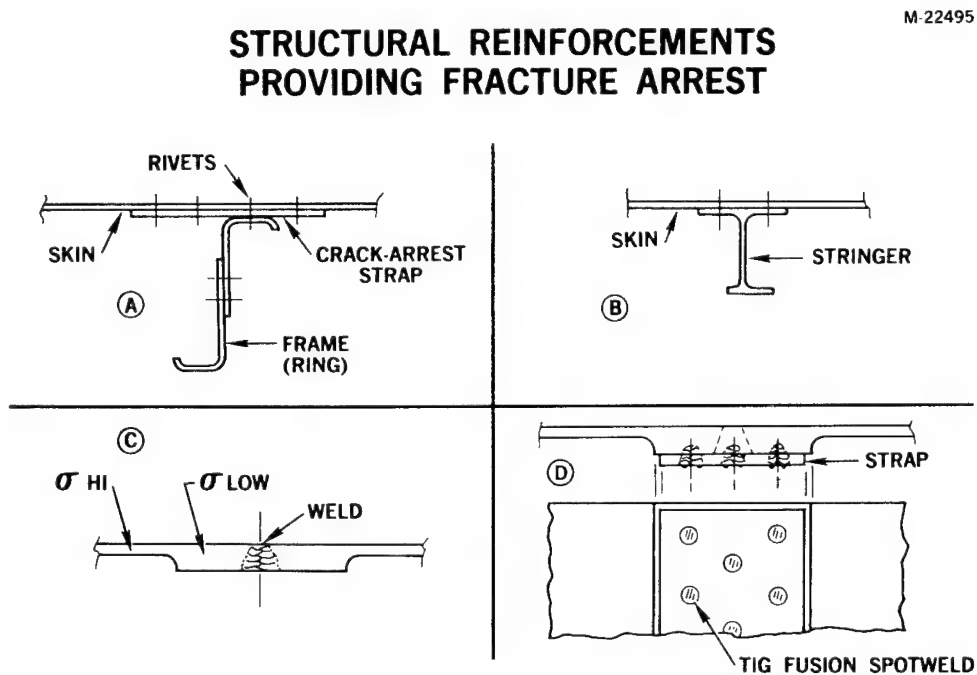
M-22495

STRUCTURAL REINFORCEMENTS
PROVIDING FRACTURE ARREST

RIVETS

SKIN

CRACK-ARREST STRAP

(A)

FRAME (RING)

SKIN

STRINGER

(B)

(C)

σ HI σ LOW

WELD

(D)

STRAP

TIG FUSION SPOTWELD

Figure E4

M-22502

Ar (AREA, STRUCTURAL REINFORCEMENT)

F

t

L

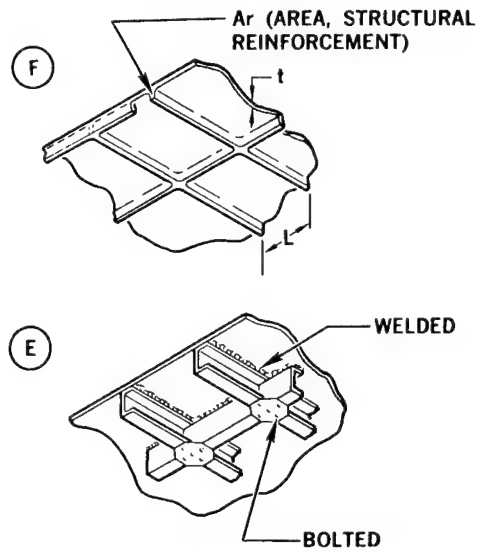**STRUCTURAL REINFORCEMENTS PROVIDING FRACTURE ARREST**

E

WELDED

BOLTED

Figure E4 (cont)

APPENDIX F

VARIABILITY OF FATIGUE CHARACTERISTICS

The fatigue property of a metal or a structure is not an absolute mechanical property. It has no fixed value and can be altered drastically by small changes in one of the many variables producing the phenomenon. This makes the calculation of an accurate prediction for the time-of-occurrence of fatigue extremely difficult and often questionable.

It is generally recognized that a large variability occurs in the test results of even the most carefully controlled research or structural development fatigue research programs. However, it is not the intent of this section to discuss the mechanisms by which various parameters quantitatively affect fatigue life variability. Rather, the intent is to shed some knowledge concerning typical trends in fatigue-life scatter. This knowledge has been determined from laboratory observations and is believed to be of use in guiding the designer.

The characteristic fatigue behavior of structure is illustrated in a qualitative manner in the following diagrams.

Figure F1 shows the life scatter in fatigue as a function of stress level. As the level of stress in a structure diminishes, the variability in the time required to produce rupture increases. The same rule also applies if the stress range of the cyclic alternation in stress diminishes. Furthermore, fatigue-life variability decreases as the severity of the stress concentrations in a structure increases. These differences are depicted in Figure F1, which also shows that severely notched members possess less scatter in life than unnotched members. Similar characteristics are evidenced in the phenomenon of fatigue-crack growth. Figure F2 depicts the growth of cracks with cycles of straining.

For purposes of simplification, metal fatigue may be considered as a two-stage process. The first stage, termed a damage nucleation period, is difficult to define in engineering terminology but has been observed to be largely responsible for the scatter in fatigue results. The life variability in the

LIFE VARIABILITY IN FATIGUE
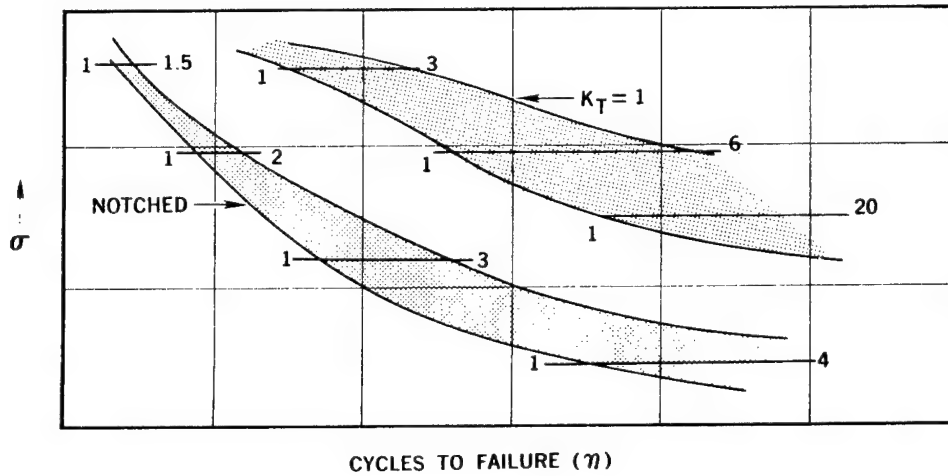## TEST RESULTS

M-22509

CYCLES TO FAILURE (n)

Figure F1

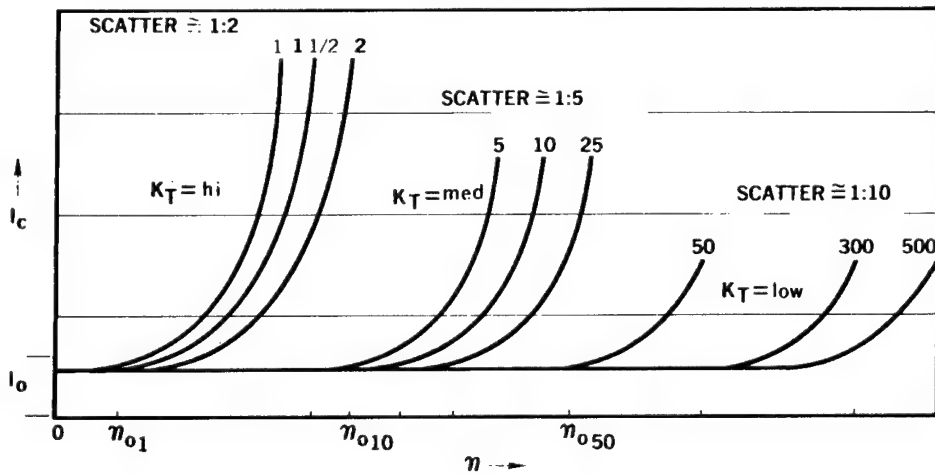# SCATTER OF FATIGUE CRACK
GROWTH CHARACTERISTICS

M-22492

Figure F2

100

second stage, termed the crack propagation period, is easily monitored and is known to be relatively small. Therefore, it can be concluded that the scatter in fatigue test results is associated mainly with the incubation stage or first stage of the fatigue phenomenon. Structures relatively free of stress concentrations have longer lives, longer damage nucleation periods, shorter crack propagation periods, and correspondingly greater variability in life than structures possessing severe stress raisers. Conversely, severely notched parts possess relatively short damage incubation periods, long crack propagation periods, and small scatter records, as has been shown in the results of replicate tests.

If the experimental data in Figure F2 for structure possessing high stress concentrations were replotted as the time required to grow a crack from its first detectable length, the variability in life is further reduced. The data in Figure F2 have been normalized and replotted in Figure F3. A practical value for the length of crack that can be detected in service is 1/8 in. to 1/4 in.
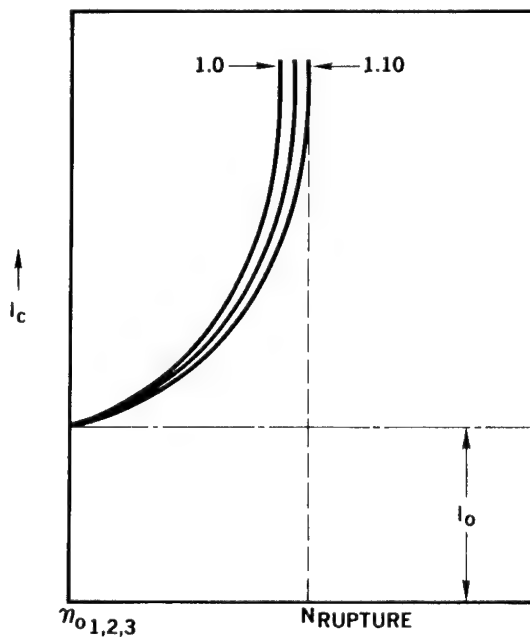

Figure F3

In the figures, this is identified as ℓ_o, which is witnessed at n_p cycles. A normal scatter of 3:1 in overall fatigue life may be reduced to a 10% scatter in behavior, if only the crack propagation period is considered. These characteristics suggest that separate probability analyses should be made for each stage of the fatigue damaging process.

APPENDIX G

SOME RECOMMENDED AREAS FOR RESEARCH IN
FATIGUE AND FRACTURE OF METALS

The principal areas in which knowledge of fatigue and fracture characteristics
of metals and structures is limited are listed below. These areas will have
to be researched before the most serviceable fatigue- and fracture-safe de-
sign criteria can be formulated for near-future aircraft and space-vehicle
structures. The status of programs now underway to study these areas
indicates that the situation will not change appreciably in the coming year.
However, the need for this knowledge is so pressing that it seems appropriate
to periodically review and update the list of material research programs that
should be undertaken. Without such reviews, the independent researchers
have little guidance in selecting areas where their particular talents can best
be applied. It is hoped that this approach will result in more useful design
data on current materials and new data on some metals that otherwise would
remain unexploited.

o   Rate of Flaw Growth in Monocoque Pressure Vessels and Tubing
     Data on the rate of crack growth in metals are predominantly for
     cases of uniaxial cyclic straining. These data are inappropriate
     for the design of multiaxially loaded structure. More programs
     are needed to obtain multiaxial information, since most structures
     are subjected to complex straining.

Figure G1 graphically depicts one approach to meet these needs. For
example, many structures are subjected to initial proofing programs. The
number of proof loadings (n_c) should be accounted for in the design. In
addition, the anticipated operational cycles must be considered. Their
continued effects (at Σn_o) can then be used to establish safe design working
stresses. The margin for safety in this case is based on the proper selection
of a working stress to meet the required useful life of the structure.

Fatigue Life and Crack Growth in Metals as a Function of Anisotropy
Large differences in residual strength and crack-growth rates have
been noted in the few observations made of these characteristics as
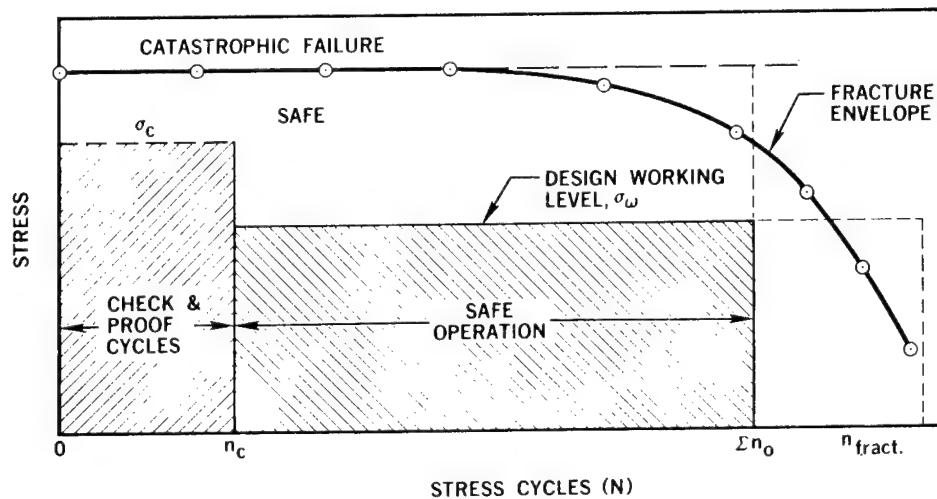
STRENGTH OF STRUCTURE AS A FUNCTION OF LIFE

Figure G1

functions of the orientation of the principal straining to the rolling direction of the material. These differences should be determined for most metals if safe design working stresses are to be defined. Some preliminary results are described in Appendix C.

- Fatigue Life as a Function of Environment
  More investigations are needed to explore the time-dependent characteristics of fatigue and fracture phenomena. Tests are required to determine the effects of inert gases, ozone, corrosive gases, liquid metals, vacuum, irradiation, and combinations of these at elevated, high, and cryogenic temperatures. Long-time as well as short-time exposure periods should also be investigated.

- Fail-Safe and Fracture-Safe Design
  The leak-before-rupture design philosophy used in aircraft may be appropriate for some spacecraft structures but not for others. Additional studies are needed in this field to define those vehicle categories which are and are not applicable.

It is recommended that future work be directed to analytical and experimental programs defining the structural stiffening requirements and stress field gradients for arresting fracture after its initiation. This should be done for integrally stiffened structure

(Figure E4 - G2), which for various reasons is a promising candi-
date for both internally pressurized space cabins and externally
pressurized submersible structures.

- Safe-Life and Crack-Free Design
  Although the philosophy of safe-life design has not proved too
  successful in aircraft, there may be some space-vehicle structure
  for which it is appropriate. Design requirements for increased
  safety of structures that have no tolerance for cracks (crack-free
  structure) will probably demand minimally stressed, greater weight
  components in some areas. Programs are needed to define thresh-
  old levels of working stress where no cracks are generated through-
  out the useful life of the structure.

- Scale Effects and Effect of Curvature
  Most experiments have been conducted on relatively small, flat test
  panels. No adequate scaling laws exist for the prediction of behavior
  of large vehicles from the test results of smaller sections. Similarly,
  the complex stress states caused when curved panels are loaded are
  not adequately accounted for in analysis. More investigations are
  required to establish scaling laws and to predict the behavior of
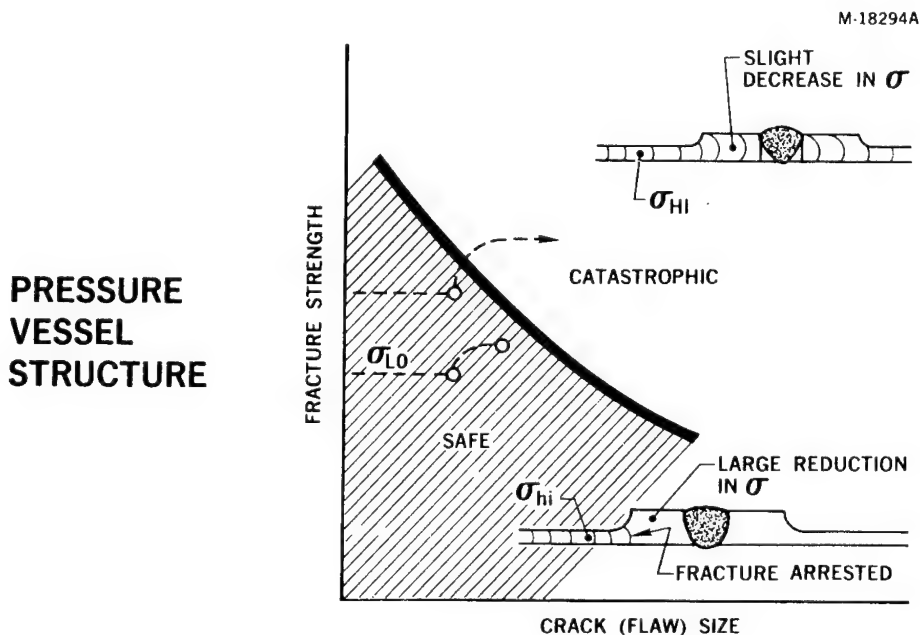 flawed pressure vessels (curved panels).

M-18294A

PRESSURE
VESSEL
STRUCTURE

Figure G2

105

- Out-of-Phase Cyclic Loading

  Many structures are subjected to a variety of cyclic loading patterns from various load sources. The straining directions within the various loading sources are seldom about the same stress axes. The accumulation of damage during cyclic straining consequently would be different for each loading source This accumulation probably has an appreciable effect on the resultant fatigue life of a structure. Although these are realistic conditions for cyclically loaded structure, no investigations yet have been attempted.

- Fracture Characteristics under Hypervelocity Impact

  Knowledge of the effect of flaws generated by hypervelocity impact and penetration on brittle materials is required for establishing related design data. It has not been demonstrated that normal fracture-mechanics theories will apply to the instantaneous stress state at a flaw produced in this manner.

  Flaws generated by meteoroid impact or penetration can be nucleii for fatigue crack growth. This subject also requires investigation.

REFERENCES

1. Symposium Proceedings of the Fatigue of Aircraft Structures. Tech. Doc. Rpt., WADC TR 59-507, August 1959.

2. Acoustical Fatigue. ASTM, Special Tech. Pub. No. 284, March 1961.

3. WADC - University of Minnesota Conference on Acoustical Fatigue. Tech. Doc. Rpt., WADC TR 59-676, March 1961.

4. Investigation of Thermal Effects on Structural Fatigue. Tech. Doc. Rpt., WADD TR 60-410 Part I and II, August 1960.

5. Symposium on Fatigue of Aircraft Structures. ASTM, Spec. Tech. Pub. No. 274, June 1960.

6. Fatigue of Aircraft Structures. ASTM STP 203, November 1956.

7. 1960: References on Fatigue. ASTM STP 9-L, July 1962.

8. Fatigue, Five Year Bibliography 1950 to 1954. ASTM STP 9AA, April 1963.

9. Symposium on Fatigue, with Emphasis on Statistical Approach - Vol. II. ASTM STP 137, February 1953.

10. Manual on Fatigue Testing. ASTM STP 91, December 1949.

11. A Guide for Fatigue Testing and the Statistical Analysis of Fatigue Data. ASTM STP 91-A, July 1963.

12. Fatigue Tests of Aircraft Structures: Low-Cycle, Full-Scale, and Helicopters. ASTM STP 338, September 1963.

13. Large Fatigue Testing Machines and Their Results. ASTM STP 216, January 1958.

14. The International Conference on Fatigue of Metals. IME and ASME, London and New York, September and November 1956.

15. J. Padlog and A. Schmitt: A Study of Creep, Creep-Fatigue, and Thermal Stress Fatigue in Airframes Subject to Aerodynamic Heating. WADC TR 58-294, July 1958.

16. Colloquium on Fatigue. Springer-Verlag O.H.G., Berlin, 1956.

17. Sines and Waisman: Metal Fatigue. McGraw Hill, 1959.

18. A.L. Eshleman; J.D. Van Dyke, Jr.; and P.M. Belcher: A Procedure for Designing and Testing Aircraft Structure Loaded by Jet-Engine Noise. Douglas Engineering Paper No. 693, March 1959.

19. G.F. Deneff: Fatigue Prediction Study. WADD TR 61-153, May 1961.

20. An Engineering Evaluation of Methods for the Prediction of Fatigue Life in Airframe Structures. Lockheed Aircraft Corp., ASD-TR-61-434, March 1961.

21. Effect of Compressive Loads on Structural Fatigue at Elevated Temperature. Douglas Aircraft Co. ASD-TR-61-434, March 1962.

22. C.M. Harris and C.E. Crede: Shock and Vibration Handbook. Vol. 1 and 2, McGraw Hill, 1961.

23. B.F. Langer: Fatigue Failure from Stress Cycles of Varying Amplitude. J. Appl. Mechanics, December 1937, p. A160.

24. R.H. Christensen: Damage Effect in Fatigue. Douglas Report STR 9564, November 1944.

25. R.H. Christensen: Cumulative Damage in Fatigue of Steel. Douglas Report STR 9656, December 1944.

26. A.K. Head and F.H. Hooke: Random Noise Fatigue Testing, International Conference on Fatigue of Metals. I.M.E. and A.S.M.E., New York and London, September 1956.

27. D.L. Henry: A Theory of Fatigue Damage Accumulation in Steel. Trans. ASME, Vol. 77, August 1955, pp. 913-918.

28. F.H. Vitovec and B.J. Lazan: Fatigue Creep, and Rupture Properties of Heat Resistant Materials. WADC TR 56-181, August 1956.

29. R.L. Orr; O.D. Sherby, and J.E. Dorn: Correlation of Rupture Data for Metals at Elevated Temperatures. Trans. ASM, V46, 1954.

30. Crack Strength and Crack Propagation Characteristics of High Strength Metals. Douglas Aircraft Co., ASD-TR-61-207, January 1962.

31. Notch Resistance and Fracture Toughness Characteristics of High Strength Metals. Douglas Aircraft Co. ASD-TDR-63-494, September 1963.

32. P. Kuhn: Notch Effects on Fatigue and Static Strength. Presented at Symposium on Aeronautical Fatigue, Rome, April 1963.

33. George C. Marshall S.F.C. Preliminary Vibration, Acoustic, and Shock Specifications for Components on Saturn IB Vehicle. IN-P&VE-S-63-1.

34. George C. Marshall S.F.C. Preliminary Vibration, Acoustic, and Shock Specifications for Components on Saturn V Vehicle. IN-P&VE-S-63-2.

35. R.H. Christensen: Environmental Effects on Fatigue Strength of Metals. Douglas unpublished report, 1963.

36. R.H. Christensen: Fatigue of Metals Accelerated by Prolonged Exposure to High Vacuum. ASM, Trans. Quart., June 1964, p. 373.

37. Crack Propagation and Crack-Stopper Techniques for Stiffened and Unstiffened Flat Sheet in a Supersonic Transport Environment. Douglas Aircraft Co. ASD-TDR-63-733, September 1963.

38. G.E. Bockrath: Master Fatigue Curves. ASM Western Metals Congress, ASTM Meeting, Los Angeles, California, March 1961.

39. J.C. McClymonds and J. K. Ganoung: Combined Analytical and Experimental Approach for Designing and Evaluating Structural Systems for Vibration Environments. 34th Shock, Vibration, and Associated Environments, Fort Ord, California, October 1964.

40. H.R. Spence and H.N. Luhrs: Structural Fatigue under Combined Random and Swept Sinusoidal Vibration. Journal of the Acoustical Society of America, Vol. 34, No. 8., August 1962.

41. P. Shahinian and M.R. Achter: Proceedings of the Crack Propagation Symposium. Vol. 1, Cranfield, England, September 1961.

"The aeronautical and space activities of the United States shall be conducted so as to contribute . . . to the expansion of human knowledge of phenomena in the atmosphere and space. The Administration shall provide for the widest practicable and appropriate dissemination of information concerning its activities and the results thereof."

—NATIONAL AERONAUTICS AND SPACE ACT OF 1958

NASA SCIENTIFIC AND TECHNICAL PUBLICATIONS

TECHNICAL REPORTS: Scientific and technical information considered important, complete, and a lasting contribution to existing knowledge.

TECHNICAL NOTES: Information less broad in scope but nevertheless of importance as a contribution to existing knowledge.

TECHNICAL MEMORANDUMS: Information receiving limited distribution because of preliminary data, security classification, or other reasons.

CONTRACTOR REPORTS: Technical information generated in connection with a NASA contract or grant and released under NASA auspices.

TECHNICAL TRANSLATIONS: Information published in a foreign language considered to merit NASA distribution in English.

TECHNICAL REPRINTS: Information derived from NASA activities and initially published in the form of journal articles.

SPECIAL PUBLICATIONS: Information derived from or of value to NASA activities but not necessarily reporting the results of individual NASA-programmed scientific efforts. Publications include conference proceedings, monographs, data compilations, handbooks, sourcebooks, and special bibliographies.

Details on the availability of these publications may be obtained from:

SCIENTIFIC AND TECHNICAL INFORMATION DIVISION

NATIONAL AERONAUTICS AND SPACE ADMINISTRATION

Washington, D.C. 20546